Atmospheric
Chemistry
and Physics

Elucidating the mechanisms of atmospheric new particle formation in the highly polluted Po Valley, Italy

Jing Cai[1], Juha Sulo[1], Yifang Gu[1], Sebastian Holm[1], Runlong Cai[1], Steven Thomas[1],
Almuth Neuberger[2,3], Fredrik Mattsson[2,3], Marco Paglione[4], Stefano Decesari[4], Matteo Rinaldi[4],
Rujing Yin[1], Diego Aliaga[1], Wei Huang[1], Yuanyuan Li[1,5], Yvette Gramlich[2,3], Giancarlo Ciarelli[1],
Lauriane Quéléver[1], Nina Sarnela[1], Katrianne Lehtipalo[1,6], Nora Zannoni[4], Cheng Wu[7], Wei Nie[5],
Juha Kangasluoma[1], Claudia Mohr[8,9], Markku Kulmala[1,5,10], Qiaozhi Zha[1,5], Dominik Stolzenburg[1,11],
and Federico Bianchi[1]

[1]Institute for Atmospheric and Earth System Research, Faculty of Science,
University of Helsinki, 00014 Helsinki, Finland
[2]Department of Environmental Science, Stockholm University, 11418 Stockholm, Sweden
[3]Bolin Centre for Climate Research, 11418 Stockholm, Sweden
[4]National Research Council of Italy – Institute of Atmospheric Sciences and Climate (CNR-ISAC),
40129 Bologna, Italy
[5]Laboratory of Atmospheric and Earth System Research, School of Atmospheric Sciences,
Nanjing University, Nanjing, 210023, China
[6]Finnish Meteorological Institute, 00560 Helsinki, Finland
[7]Department of Chemistry and Molecular Biology, Atmospheric Science,
University of Gothenburg, 41296 Gothenburg, Sweden
[8]Laboratory of Atmospheric Chemistry, Paul Scherrer Institute, 5232 Villigen, Switzerland
[9]Department of Environmental System Science, ETH Zurich, 8092 Zurich, Switzerland
[10]Beijing Advanced Innovation Center for Soft Matter Science and Engineering,
Beijing University of Chemical Technology, Beijing, 100029, China
[11]Institute for Materials Chemistry, TU Wien, 1060 Vienna, Austria

Correspondence: Dominik Stolzenburg (dominik.stolzenburg@tuwien.ac.at) and Federico Bianchi
(federico.bianchi@helsinki.fi)

Abstract. New particle formation (NPF) is a major source of aerosol particles and cloud condensation nuclei in the troposphere, playing an important role in both air quality and climate. Frequent NPF events have been observed in heavily polluted urban environments, contributing to the aerosol number concentration by a significant amount. The Po Valley region in northern Italy has been characterized as a hotspot for high aerosol loadings and frequent NPF events in southern Europe. However, the mechanisms of NPF and growth in this region are not completely understood. In this study, we conducted a continuous 2-month measurement campaign with state-of-the-art instruments to elucidate the NPF and growth mechanisms in northern Italy. Our results demonstrate that frequent NPF events (66 % of all days during the measurement campaign) are primarily driven by abundant sulfuric acid (8.5×10^6 cm^{-3}) and basic molecules in this area. In contrast, oxygenated organic molecules from the atmospheric oxidation of volatile organic compounds (VOCs) appear to play a minor role in the initial cluster formation but contribute significantly to the consecutive growth process. Regarding alkaline molecules, amines are insufficient to stabilize all sulfuric acid clusters in the Po Valley. Ion cluster measurements and kinetic models suggest that ammonia (10 ppb) must therefore also play a role in the nucleation process. Generally, the high formation rates of sub-2 nm particles (87 cm^{-3} s^{-1}) and nucleation-mode growth rates (5.1 nm h^{-1}) as well

as the relatively low condensational sink ($8.9 \times 10^{-3}\,\mathrm{s}^{-1}$) will result in a high survival probability for newly formed particles, making NPF crucial for the springtime aerosol number budget. Our results also indicate that reducing key pollutants, such as SO_2, amine and NH_3, could help to substantially decrease the particle number concentrations in the Po Valley region.

1 Introduction

New particle formation (NPF) occurs ubiquitously in the troposphere and affects the global climate (Dunne et al., 2016) and local or regional air quality (Kulmala et al., 2021). NPF and further growth of the newly formed particles dominate aerosol number concentrations and are the major contributor to the ultrafine (< 100 nm) aerosol budget, which poses a significant health threat to the population in polluted areas (Schraufnagel, 2020). While air pollution mitigation strategies mostly focus on reducing particulate mass (particulate matter below $2.5\,\mu\mathrm{m}$ – $PM_{2.5}$), ultrafine particle number concentrations might not be affected by such policies (de Jesus et al., 2019). It is, therefore, essential that we understand the mechanisms leading to NPF in polluted environments to design better-targeted air quality strategies for polluted European regions, where $PM_{2.5}$ reduction measures are already implemented.

NPF is closely linked to atmospheric air pollution. Efficient nucleation and growth are crucial factors contributing to haze formation, accounting for over 65 % of the particle number concentration in urban environments (Kulmala et al., 2021; Guo et al., 2014; Chu et al., 2019; Sebastian et al., 2022). Strong and frequent NPF events have been reported in the most urbanized areas of China, such as the North China Plain (Wang et al., 2013, 2015; Wu et al., 2007, 2011; Shen et al., 2011), the Yangtze River Delta (Dai et al., 2017; Yu et al., 2016; Xiao et al., 2015) and the Peal River Delta (Yue et al., 2013; Peng et al., 2014; Liu et al., 2008). This observation contradicts theoretical calculations which suggest that NPF events are less likely to occur in polluted areas, where high levels of pre-existing aerosols acting as condensation sinks (CSs) are capable of quickly scavenging gaseous precursors of NPF (Kulmala et al., 2017).

The elucidation of NPF precursors and mechanisms has varied among different sampling locations and studies. Currently, no uniform theory or mechanism can elucidate NPF occurrence in different polluted areas or in different seasons. For example, in Shanghai and Beijing (China), sulfuric acid (SA, H_2SO_4) and amines have been identified as key contributors to initial particle formation (Yao et al., 2018; Cai et al., 2021; Yan et al., 2021). On the other hand, some studies have also suggested that photooxidation products of vehicle-emitted organic vapors dominate NPF under urban conditions, rather than SA or basic species (Guo et al., 2020). Meanwhile, in Barcelona (Spain), which is significantly less polluted than Asian megacities but still shows

frequent high pollution levels, NPF has been reported to be associated with SA along with highly oxygenated organic molecules (HOMs) (Brean et al., 2020). These discrepancies in the reported NPF mechanisms may arise from the limited utilization of state-of-the-art instruments, such as those capable of measuring size distributions down to 1–2 nm as well as directly identifying clusters and vapors, which are influenced by spatiotemporal variations (Wang et al., 2017). Therefore, gaining a better knowledge of the key participants, nucleation mechanisms and roles of pre-existing particles is crucial for comprehending the causes of the high NPF frequencies in polluted regions. This knowledge can be essential for developing effective local $PM_{2.5}$ control and implementation strategies.

The Po Valley region is one of the most important industrial and agricultural areas in southern Europe with dense population (> 17 million people per $70\,000\,\mathrm{km}^2$). It is located in northern Italy, surrounded by the Alps (in the north), the Apennine Mountains (in the south) and the Adriatic Sea (in the east). High primary anthropogenic emissions; a mixture of numerous pollutants from industrial, urban and agricultural sources; and frequently occurring stagnant meteorological conditions in winter make the Po Valley region a European hotspot with respect to high aerosol loadings (Saarikoski et al., 2012; Li et al., 2014; Finzi and Tebaldi, 1982; Daellenbach et al., 2023). However, this region is distinct from Asian megacities in that the population density is significantly lower (250 people km^{-2} in the Po Valley compared with, e.g., 1400 people km^{-2} in Beijing), resulting in effects such as traffic or residential heating being less dominant pollution sources. At the same time, NPF occurs frequently in the Po Valley (Hamed et al., 2007; Manninen et al., 2010). For example, Shen et al. (2021) observed that NPF events took place on approximately 70 % of the days during spring and summer. Similarly, Kontkanen et al. (2017) discovered that NPF occurred on 89 % of the days during summer. During NPF event days, high formation rates of sub-2 nm neutral particles (J_2, $\sim 10^1$ to $10^2\,\mathrm{cm}^{-3}\,\mathrm{s}^{-1}$; Kontkanen et al., 2017) and SA concentrations ($\sim 1 \times 10^7\,\mathrm{cm}^{-3}$) were observed in the Po Valley (Paasonen et al., 2010; Kontkanen et al., 2017). These levels were among the highest recorded in a study conducted at nine sites across the Northern Hemisphere (Kontkanen et al., 2017).

While previous studies conducted in the Po Valley have reported frequent NPF events characterized by high nucleation and growth rates, the clustering mechanism and the dominant precursors for particle growth have not been inves-

tigated to date. Specifically with respect to the distinct features of the Po Valley compared with the more intensely researched megacity environments, a deeper understanding of frequent NPF events, including their precursors, nucleation mechanisms and growth processes, is crucial for air pollution control and the effective implementation of $PM_{2.5}$ mitigation measures in such a semi-urban but highly industrialized region. In this study, we conducted a 2-month field campaign in the months of March and April 2022. During this field campaign, we (1) identified the chemical composition of atmospheric neutral and ion clusters using a set of state-of-the-art mass spectrometers, (2) characterized the initial NPF and further growth rates using particle number size distribution measurements down to 1 nm, and (3) compared the field measurement results with the recent Cosmics Leaving Outdoor Droplets (CLOUD) chamber experiments to investigate the mechanism of NPF events in the Po Valley region. This allowed us to elucidate the NPF and growth mechanisms at a polluted southern European site and to give insights into the best mitigation strategies for ultrafine particle pollution in the context of already implemented $PM_{2.5}$ reduction strategies.

2 Method

2.1 Measurement site

Our measurement was part of the Fog and Aerosol InterRAction Research Italy (FAIRARI) field campaign in San Pietro Capofiume (SPC; 44.65° N, 11.62° E; 5 m a.s.l., meters above sea level), located in the Po Valley region in northern Italy. The measurement site is part of the Aerosol, Clouds and Trace Gases Research Infrastructure (ACTRIS) Italy network and is operated by the National Research Council of Italy – Institute of Atmospheric Sciences and Climate (CNR-ISAC). The SPC site is approximately 30 km northeast of Bologna (population of $\sim 400\,000$) and 20 km south of Ferrara (population of $\sim 130\,000$), the two major cities in the area. The distance from the measurement site to the Adriatic Sea (to the east) is about 50 km. The area around the sampling site consists of agricultural fields, a smaller town (population of < 2000, within 5 km) and smaller settlements in close proximity. Given its location, the SPC rural station is considered to be representative of the regional background of the Po Valley (Paglione et al., 2020, 2021; Paasonen et al., 2010; Hamed et al., 2007; Saarikoski et al., 2012; Decesari et al., 2014). The instruments for the NPF measurement were operated in a temperature-controlled ($\sim 20\,°C$) container from 1 March to 30 April 2022.

During the sampling period, the daily average temperature ranged from 1 to 17 °C. The average wind speed (WS) was approximately $2.4 \pm 1.5\,\mathrm{m\,s^{-1}}$ (Fig. 1b). The average WS in the daytime was $3.5\,\mathrm{m\,s^{-1}}$ from the east, which was significantly higher than the wind at night ($1.5\,\mathrm{m\,s^{-1}}$) that blew from the west. Strong diurnal variation in the wind direction was observed, typically from the west at night to the east dur-

ing the day (Fig. 1a). This pattern was potentially influenced by the sea–land breeze from the Adriatic Sea. Accordingly, the daily average relative humidity (RH) varied from 41 % to 98 %, with values as high as 85 % at night that sharply decreased to around 40 % at noon due to the strong temperature variation.

2.2 Instruments

2.2.1 Chemical composition measurements

The chemical composition of cluster ions was measured using a high-resolution atmospheric-pressure-interface time-of-flight mass spectrometer (APi-ToF, Aerodyne Research Inc. and Tofwerk AG). The APi-ToF measures naturally charged ions in the ambient environment. A detailed description of the instrument can be found in Junninen et al. (2010). In this study, ambient air was sampled through a 0.57 m stainless-steel tube with a flow rate of $\sim 10\,\mathrm{L\,min^{-1}}$ (LPM), with 0.8 LPM of the sample flow entering the APi-ToF.

The concentration of SA was measured using a nitrate-ion-based (NO_3^--based) chemical-ionization (CI) atmospheric-pressure-interface time-of-flight mass spectrometer (CI-APi-ToF, Aerodyne Research Inc. and Tofwerk AG; Jokinen et al., 2012). The CI-APi-ToF is an APi-ToF coupled with a CI unit, equipped with a soft X-ray source (L9490, Hamamatsu Photonics, 9.5 kV) to produce the primary ions. The sampling flow went into the instrument through a $\sim 0.6\,\mathrm{m}$ (0.75 in.) stainless-steel tube. The sampling flow was 10 LPM and the sheath flow was set to 20 LPM. Data acquisition for CI-APi-ToF was performed with a time resolution of 10 s. A calibration factor of $1.0 \times 10^{10}\,\mathrm{cm^{-3}}$ for SA was determined with sampling loss corrections before the campaign according to the method proposed by Kurten et al. (2012).

Dimethylamine (DMA) measurements were performed with a Vocus CI-ToF (time-of-flight) mass spectrometer (hereafter Vocus, Aerodyne Research Inc. and Tofwerk AG) using H_3O^+ as a reagent ion. The Vocus has been described in detail in Krechmer et al. (2018), and the study by Wang et al. (2020) utilized a Vocus instrument for DMA observations. In this study, the focusing ion-molecule reactor (FIMR) of the Vocus instrument operated at a pressure of 2.0 mbar and a temperature of 100 °C with a radio frequency amplitude of 350 V and a frequency of 1.4×10^6 Hz. Data acquisition was performed with a time resolution of 10 s in the atomic mass unit range of 0–1000 amu.

2.2.2 Particle size distribution measurements

Particle size magnifier

The Airmodus A11 nano-CNC (nano condensation nucleus counter) system, colloquially known as the particle size magnifier (PSM), is a two-step condensation particle counter (CPC) capable of measuring particle size distributions of sub-3 nm particles (Vanhanen et al., 2011). The sys-
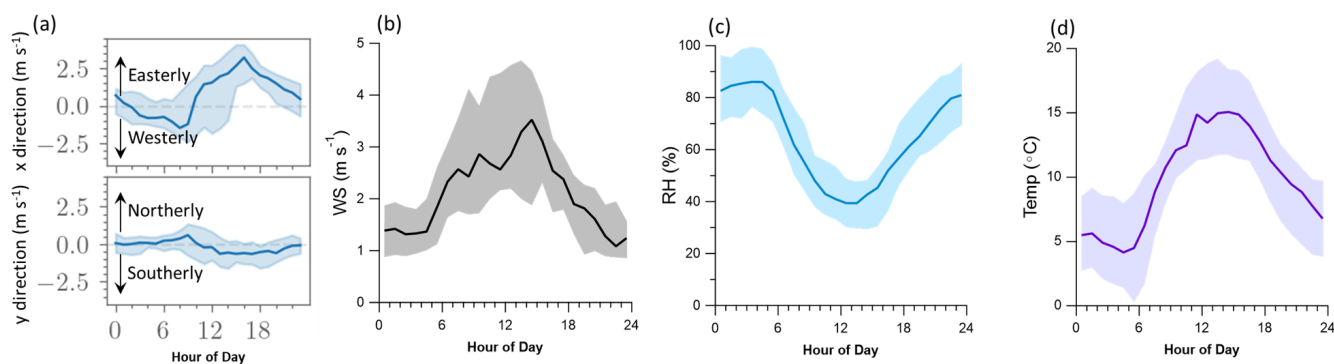
Figure 1. Diurnal variation in **(a)** average wind vectors, **(b)** wind speed, **(c)** relative humidity (RH) and **(d)** temperature. The shaded areas present the 25th and 75th percentiles.

tem consists of two parts, in which the PSM (Airmodus A10) acts as a preconditioner where particles are grown first before being funneled to the CPC (Airmodus A20) for further growth and optical detection. In the PSM, the sample flow is turbulently mixed with a heated flow saturated with diethylene glycol (DEG) in the mixing section, and the DEG then condenses on the particles in the growth tube. By scanning the flow rate through the DEG saturator, the smallest activated particle size is altered which can be converted into a sub-3 nm particle size distribution. Further particle growth is achieved by butanol in the CPC such that the particles reach optically detectable sizes.

The PSM was calibrated according to the standard operation procedure for PSM (Lehtipalo et al., 2022) using a known aerosol population from a glowing-tungsten-wire generator (Kangasluoma et al., 2015; Peineke et al., 2006). The detection efficiency for different particle sizes was determined by comparing the concentration of size-selected particles to a reference instrument, in this case a Faraday cup electrometer.

The system was set up with an Airmodus nanoparticle diluter (AND) inlet (Lampimäki et al., 2023) for sample dilution and automatic background measurement to make sure that the CPC stayed within a single counting range during the campaign. The inlet was set up at around 2 m above the ground, and the background was measured roughly every 8 h and subtracted from the signal during the inversion process.

High-flow differential mobility particle sizer (HFDMPS) and Hauke-type DMPS

The high-flow differential mobility particle sizer (HFDMPS) system utilizes a half-mini differential mobility analyzer (DMA; Fernández de la Mora and Kozlowski, 2013; Cai et al., 2018) to size-select particles that are then grown and detected by an A11 nano-CNC system (Airmodus Ltd.; Kangasluoma et al., 2018). The HFDMPS significantly improves sub-10 nm particle measurements compared with a typical differential mobility particle sizer (DMPS) system,

allowing us to better characterize the sub-10 nm particle size distribution when combined with the PSM measurements. The DMA was size-calibrated with electro-sprayed positively charged monomer ions of tetraheptylammonium bromide (THA+; Ude and de la Mora, 2005).

The HFDMPS inlet was set up at a height of 1 m and used a 50 cm long, 10 mm outer diameter tube with a core sampling system to minimize losses (Kangasluoma et al., 2016; Fu et al., 2019). A home-built soft X-Ray ionization source (similar to the Model 3087, TSI Inc.) was used to charge particles. The HFDMPS measured the particle size distribution from 2 to 15 nm for both polarities at 15 predefined size steps within 10 min.

Sampling from the same inlet and using the same charging device, a conventional DMPS system equipped with a Hauke-type DMA (aerosol flow 1 LPM, sheath flow 5 LPM) and a TSI Inc. CPC (Model 3772) measured the particle size distribution from 10 to 800 nm at 16 predefined size steps within 10 min. In addition, a DMPS measuring from 15 to 800 nm was available in another measurement container at the same field site. The total particle number concentrations obtained from integrating the particle size distribution measured by the DMPS was compared with a reference CPC (Model 3025A, TSI Inc.) operated at the same site during the first weeks of the campaign. It revealed, on average, a factor of 2 lower concentrations measured by the Hauke-type DMPS that was confirmed to be rather size-independent via a comparison of the measured size distributions and their overlap with the HFDMPS system and was, thus, subsequently corrected for.

2.2.3   Co-located measurements

Additional co-located measurements of auxiliary data from the CNR-ISAC network (https://www.isac.cnr.it/en, last access: 10 February 2024) and from the routine monitoring program of the Regional Environmental Protection Agency of Emilia-Romagna (ARPA-E, https://www.arpae.it/it, last access: 10 February 2024) were used in this study. An on-

line high-resolution time-of-flight aerosol mass spectrometer (HR-ToF-AMS, Aerodyne Research) and a multi-angle absorption photometer (MAAP, Thermo Scientific) were operated at the same site for the measurement of non-refractory species and black carbon (BC), respectively. Trace gases were also measured with a 1 min time resolution, including O_3 (Model 49i, Thermo Scientific), NO_x (Model 200A, Teledyne API), NH_3 (Model 201E, Teledyne API) and SO_2 (Model 43i enhanced trace level analyzer, Thermo Scientific). Moreover, meteorological parameters (e.g., RH, temperature, wind direction and wind speed) were measured by a meteorology station (Model WXT536, Vaisala Ltd).

2.3 Data processing

2.3.1 New particle formation classification

We classified each day according to whether a growing mode appeared in the particle size distribution or not. This classification was done separately for both the HFDMPS and the PSM data. A growing mode was defined as a new particle mode that appeared in the particle size distribution and continued to grow to larger sizes for at least 2 h. If there was a growing mode visible in both the PSM and HFDMPS data, the day was defined as "NPF with growth". If there was no growth or the growth was unclear in the HFDMPS data but there was a growing mode in the PSM data, then the day was classified as "NPF with no growth". If there was no growing mode in either of the size distributions measured by HFDMPS and PSM, then the day was marked as "no NPF event" (Fig. S1 in the Supplement). The definition is similar to Dada et al. (2018), who used naturally charged ions to separate between NPF days with clustering only and those with clustering and visible growth. If there was a growing or an undefined new mode visible in the combined size distribution but there was no clustering detected by the PSM, this day was marked as "Unclear". Days that lacked data from one of the instruments were marked as "No data".

2.3.2 Condensation sink, nucleation and growth rate calculations

The condensation sink and coagulation sink were calculated according to Dal Maso et al. (2005) from the Hauke-type DMPS size distribution without any correction of aerosol hygroscopic behavior. Growth rates were calculated using the maximum concentration method, in which we fit a Gaussian distribution to the particle concentration evolution at a fixed size to determine the time of maximum concentration for a given size channel in the HFDMPS.

The growth rates (GRs) were calculated by first determining the time to reach 50 % of the maximum concentration, and the average growth rate was then derived as the slope of the linear fit between the time and diameter:

$$\text{GR} = \frac{\Delta d_p}{\Delta t} \approx \frac{d_{p,f} - d_{p,i}}{t_f - t_i}, \tag{1}$$

where $d_{p,f}$ is the diameter at the end time t_f and $d_{p,i}$ is the diameter at the start time t_i.

From these, the growth rate was calculated as the slope of a linear least-squares fit to the time points of maximum concentration and their corresponding particle diameters. The formation rates were calculated for several sizes with the balance equation of Kulmala et al. (2012) using the combined-DMPS size distributions (J_2, J_3 and J_6) and the PSM and combined-DMPS size distribution ($J_{1.7}$). Formation rates were then calculated by rearranging the equation describing the time evolution of the particle size distribution. The formation rate for a given diameter d_{p1} is calculated as follows:

$$J_{dp_1} = \frac{dN_{dp_1-dp_2}}{dt} + \text{CoagS}_{dp_1} \cdot N_{dp_1-dp_2} + \frac{\text{GR}}{\Delta d_p} N_{dp_1-dp_2}. \tag{2}$$

2.3.3 Mass spectrometer data analysis

The APi-ToF and CI-APi-ToF data were analyzed using the Tofware package (v.3.1.0, Tofwerk, Switzerland, and Aerodyne, USA) in the Igor Pro software (v.7.08, WaveMetrics, USA). The mass accuracy was within 10 ppm (APi-ToF) and 5 ppm (CI-APi-ToF), and the mass resolutions were $\sim$ 4500 (APi-ToF) and $\sim$ 5000 (CI-APi-ToF) for ions > 200 Th. The raw signals were first normalized by the primary ions (NO_3^-, monomer, dimer and trimer) and then multiplied by the calibration factor of SA. Detailed information on the mass spectrometer data analysis methods can be found in previous studies (Cai et al., 2022; J. Cai et al., 2023; Zha et al., 2018, 2023a, b; Fan et al., 2021).

2.3.4 Kinetic model simulations

In order to evaluate the contribution of SA–amine clustering to cluster formation in the Po Valley, we applied a kinetic model to simulate SA dimer concentrations. We simulated the cluster concentrations and particle formation rates under different amine levels based on the model. The simulation was performed with a temperature of 283 K, an atmospheric pressure of 1.01×10^5 Pa and a condensation sink (CS) of 0.01 s^{-1}, based on our measurement during the sampling period. In the model, the formation rate of SA tetramer was regarded as the simulated particle formation rate. The standard molar Gibbs free energy of formation and the corresponding evaporation of SA–amine clusters was based on quantum chemistry with corrections from the experimental data. The detailed settings of the kinetic model can be found in Cai et al. (2021).

3 Results and discussion

3.1 NPF event frequency in the Po Valley

During the measurement period, frequent NPF events occurred in the Po Valley (Figs. 2 and S1). On 27 % of the days, we observed NPF with growth at the site, while on
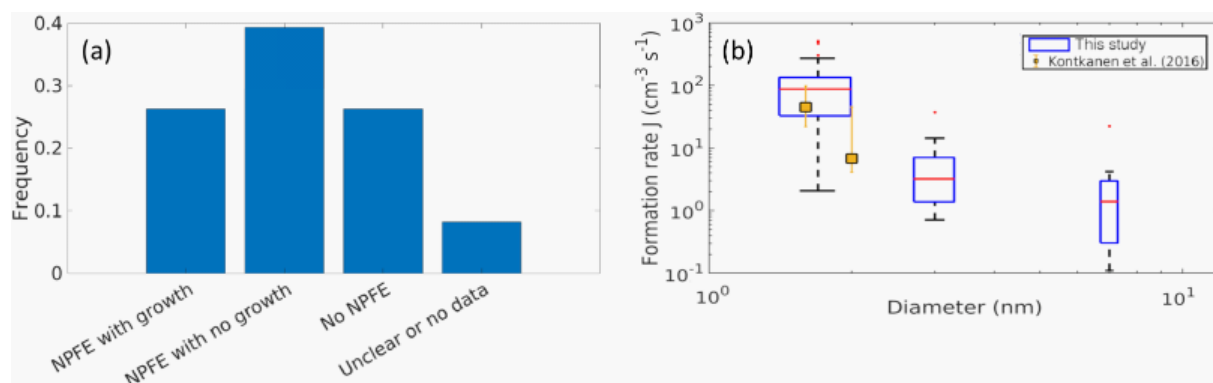
Figure 2. (a) The frequency of NPF events with and without growth, of days without NPF events, and of days with unclear classification or no data during this study. **(b)** Calculated formation rates at 1.7, 3 and 7 nm from this study and values reported by Kontkanen et al. (2016, yellow squares). The red lines are the median values of the maximum formation rates measured during an NPF event, the blue boxes show the values between the 25th and 75th percentiles, and the black whiskers mark the 5th and 95th percentiles. Red dots are outliers, and the width of the box is proportional to the square root of the number of the J values.

39 % of the days we observed NPF without growth. In total, we observed new sub-3 nm clusters forming on 66 % of the days (Fig. 2). Even though we applied a similar definition of NPF events to that used in previous work, we can only compare our NPF with growth type with the reported NPF event frequency due to the lack of capacity to measure the sub-3 nm particles in previous literature. Our results were similar to those of Hamed et al. (2007), who observed NPF events 36 % of the time in March and April of 2002 at the same site. Manninen et al. (2010) observed NPF events during more than half of all days from March to October in 2008, whereas Kontkanen et al. (2016) observed NPF during 89 % of the days in July at the same site, which is higher than our observations. Hamed et al. (2007) also observed NPF with growth events on 60 % of the days during summer, which suggests that the summertime NPF frequency at SPC is typically higher than our observation in springtime 2022. This difference in the observed NPF frequency was likely due to the different season with favorable conditions for NPF, such as a potentially lower CS (due to less stagnant meteorological conditions) and higher alkaline- and organic-molecule concentrations in summer. In addition, the abundant solar radiation and low aerosol water content (limiting surface area and heterogenous reactions; Du et al., 2022) likely create favorable conditions for NPF to occur.

The median of particle formation rate average values at 1.7, 3 and 7 nm for all sampling days with NPF with growth events were $87 \, \mathrm{cm^{-3} \, s^{-1}}$ ($32–133 \, \mathrm{cm^{-3} \, s^{-1}}$), $3.2 \, \mathrm{cm^{-3} \, s^{-1}}$ ($1.4–7.0 \, \mathrm{cm^{-3} \, s^{-1}}$) and $1.4 \, \mathrm{cm^{-3} \, s^{-1}}$ ($0.3–3.0 \, \mathrm{cm^{-3} \, s^{-1}}$), respectively, where the values in parentheses represent the respective 25th and 75th percentiles. The formation rate at 1.7 nm during NPF with growth days (NPF with growth, $87 \, \mathrm{cm^{-3} \, s^{-1}}$) is similar to that observed previously at the same site by Kontkanen et al. (2016) in summer. The high formation rate, which is comparable to heavily pol-

luted urban environments, such as Beijing and Shanghai in China ($59–225 \, \mathrm{cm^{-3} \, s^{-1}}$; Deng et al., 2020; Yao et al., 2018), will be further discussed in Sect. 3.4. The average formation rate ($J_{1.7}$) on NPF days without growth ($24 \, \mathrm{cm^{-3} \, s^{-1}}$) is much lower. During noontime, the formation rate of particles for NPF events with no growth was less than half of NPF with growth (Fig. S2). This suggests that, for particles to grow in a polluted environment such as the Po Valley, there needs to be abundant clustering to overcome losses to the existing condensation sink so that at least some of the particles survive to grow into larger sizes.

SA has long been known as a primary gaseous precursor for NPF in continental environments, owing to its extremely low volatility (Kirkby et al., 2011; Kulmala et al., 2013). During our sampling period, we observed high SA concentration in the Po Valley, in accordance with the frequent NPF events. The daily average SA concentration measured between 10:00 and 14:00 LT was $4.6 \times 10^6 \, \mathrm{cm^{-3}}$, which increased to $8.5 \times 10^6 \, \mathrm{cm^{-3}}$ during NPF events with growth, aligning with previous findings from the same site ($1.6 \times 10^7 \, \mathrm{cm^{-3}}$ during NPF in summer of 2009; Paasonen et al., 2010). Over the entire sampling period (10:00–14:00 LT), SA showed a moderate correlation with the calculated $J_{1.7}$ ($r = 0.49$, Spearman correlation coefficient, for the logarithmic values), but its relationship varied among different days. This suggests that, in addition to SA, other components, such as alkaline molecules, may also contribute to driving NPF events and subsequent growth in the Po Valley.

3.2 Nucleation mechanism

To investigate the NPF mechanism in the Po Valley, we firstly compared the simultaneously measured $J_{1.7}$ and SA with recent Cosmics Leaving Outdoor Droplets (CLOUD) chamber experiments that simulated NPF under polluted boundary layer conditions with anthropogenic emissions (Xiao et
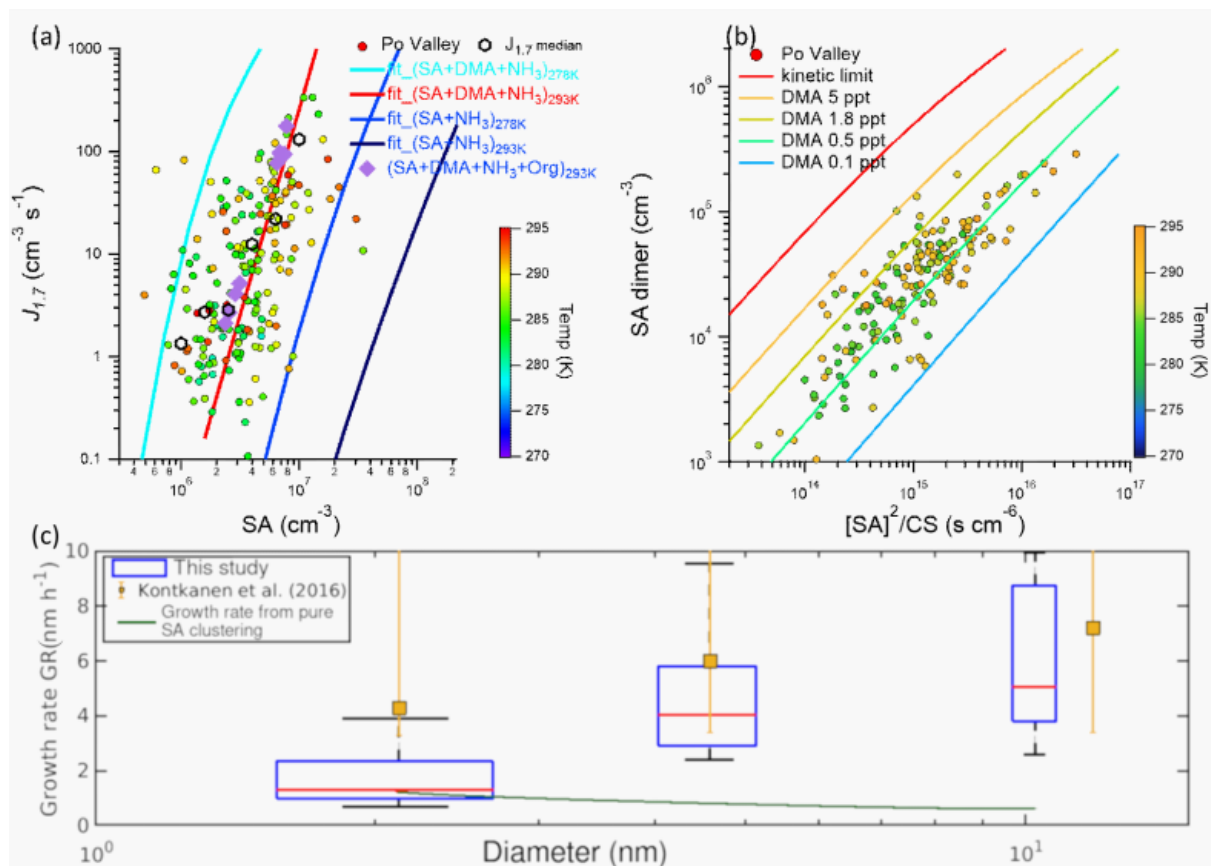
Figure 3. (a) The formation rate of 1.7 nm particles ($J_{1.7}$) versus SA concentrations during springtime in the Po Valley (shown as circles) and experimental results from CLOUD chamber experiments. The solid lines are from fitted results of CLOUD chamber experiments; the black hexagons represent the median values under different SA levels from the ambient measurement. **(b)** The relationship between the sulfuric acid dimer (SA dimer) concentration, the square of monomer $(SA)^2$ concentrations and the CS. The lines are from the kinetic model simulations under different DMA levels, whereas the dots are from the measurement. In panels **(a)** and **(b)**, the results from the field measurements are from the daytime (10:00–14:00 LT) and are color-coded by the temperature at the site. The $J_{1.7}$ and corresponding SA concentrations of CLOUD chamber results are from previous literature (Xiao et al., 2021). **(c)** Calculated growth rates for 1.5–3, 3–7 and 7–15 nm from this study and values reported by Kontkanen et al. (2016, yellow squares). The red horizontal lines are the median values, the blue boxes show the values between the 25th and 75th percentiles, and the black whiskers mark the 5th and 95th percentiles. The solid green line represents predicted growth rates from pure sulfuric acid without organic condensation (Stolzenburg et al., 2020). The width of the box is proportional to the square root of the number of the GR values.

al., 2021). In those experiments, amines, ammonia and aromatics were added to reflect an environment that was heavily influenced by anthropogenic emissions. Certain alkaline molecules, including amines (e.g., dimethylamine – DMA) and ammonia (NH_3) have been shown to substantially enhance nucleation and reduce evaporation by stabilizing atmospheric SA in chamber studies (Almeida et al., 2013). Furthermore, oxygenated organic molecules (OOMs) can also contribute to NPF and subsequent particle growth, even without the inclusion of SA (Kirkby et al., 2016; Xiao et al., 2021). As shown in Fig. 3a, most of the measurements were above the SA–NH_3 system at 278 K from the CLOUD chamber, suggesting that the SA–NH_3 mechanism itself cannot solely explain the measured $J_{1.7}$ and that other species are most likely participating in NPF in the Po Valley. For instance, amines, such as DMA or trimethylamine (TMA), with higher basicity may contribute to NPF, consistent with non-negligible concentrations of amines in previous studies in the aerosol at SPC (Paglione et al., 2014; Decesari et al., 2014). For the whole sampling period, the median SA and $J_{1.7}$ values in the Po Valley follow the SA–DMA–NH_3 (4 ppt DMA and 1 ppb NH_3) and SA–DMA–NH_3–Org (adding additional oxidized aromatic organics; Xiao et al., 2021) lines from the CLOUD chamber at 293 K, even though the average noontime temperature was around 285 K during most of the NPF days (Fig. 3a).

The SA dimer measured by CI-APi-ToF is typically used as an indicator for the initial step for the cluster formation in NPF events (Yan et al., 2021). According to a previous study (Yan et al., 2021), the source and sink terms of the SA dimer

can be determined by calculating the formation rate from SA monomer collisions and the loss rate from the SA dimer through coagulation onto pre-existing particles (Fig. 2b). In general, the correlation coefficient between the SA dimer and its source to sink term ratios ($r = 0.80$, Spearman correlation coefficient) indicated that, similar to Chinese urban areas, the SA dimer was in a pseudo-steady state between the formation of SA monomer collision and the loss onto the CS by coagulation.

To further assess the influence of DMA, one of the most common and efficient alkaline molecules for NPF in urban environments (Yao et al., 2018), we compared the measured SA dimer concentrations with the simulated values under different DMA levels (from 0.1 ppt to reaching the kinetic limit) using the kinetic model (Fig. 3b). From our cluster kinetics simulations, during the peak hours of NPF, DMA concentrations are expected to be in the range of 0.1 to 5 ppt, which is lower than the requirement to reach the kinetic limit (Figs. 3b and S3). This implies that other factors, e.g., the abundant ambient NH_3 ($\sim$ 10 ppb) or TMA during our study period, may also participate in cluster formation. This is consistent with the Vocus measurement, which suggests that the ambient DMA signals were close to the background levels (Fig. S4). Possible reasons for not reaching SA–DMA limit during the campaign could be (1) the relatively lower DMA emissions (such as vehicle flows) than those in Chinese megacities (Ge et al., 2011; Zhu et al., 2022) and (2) the quick scavenging caused by photolysis and nighttime high RH (85 %) (Leng et al., 2015; Yao et al., 2016). Therefore, both the abundant ambient NH_3 concentrations ($\sim$ 10 ppb) and amines likely participated in cluster formation during our study period.

Median particle growth rates (GRs) during NPF events for the 1.5–3, 3–7 and 7–15 nm size ranges were 1.3 (1.0–2.4) nm h^{-1}, 4.6 (2.9–5.8) nm h^{-1} and 5.1 (3.8–8.8) nm h^{-1}, respectively. The values in parentheses represent the respective 25th and 75th percentiles of data (Fig. 3c). Growth rates increase with particle diameter, which is a phenomenon also observed in other campaigns around the world (Kontkanen et al., 2017; Kulmala et al., 2013), typically indicative of an increasing organic vapor contribution with size (e.g., Stolzenburg et al., 2018). The growth rates observed here were similar to those observed by Kontkanen et al. (2016) at SPC in summer (7.2 nm h^{-1} for 7–20 nm). Moreover, our 1.5–3 nm growth rate matches well with Manninen et al. (2010) (1.5 nm h^{-1}) during spring in the Po Valley. A comparison to predicted growth rates from sulfuric acid condensation without organics, which was calculated based on kinetic collisions of the measured SA concentrations and the effect of van der Waals forces on the collision frequency (Stolzenburg et al., 2020), suggests that sulfuric acid condensation may be, on average, sufficient for the growth of the smallest clusters (Fig. 3c). This supports the argument that sulfuric acid and its stabilizing molecules (likely the bases, such as NH_3 and amines) were controlling particle formation in the

initial steps of NPF and growth in the Po Valley. However, for particles to grow beyond 3 nm in size, other vapors were needed, which was suggested by the significantly lower contribution of growth by SA (indicated by the green line) than the measured GR for 3–7 and 7–15 nm particles (Fig. 3c). Those vapors were likely a mixture of organics from anthropogenic and biogenic origins (with the latter emitted at higher rates during summer). We compared the GR during NPF with and without growth events using the method proposed in Kulmala et al. (2022): the signal was averaged for all classified non-event days and an appearance time fit was then performed for each size channel independently, also revealing a growth pattern. We found no significant difference with respect to the GR in the 7–15 nm size range for NPF with or without growth days (GR = 5.1 nm h^{-1} for NPF with growth days and GR = 6.1 nm h^{-1} for NPF without growth days). Considering the similar CS and GR levels for NPF with and without growth days, the higher formation rates at 1.7 nm (87 cm^{-3} s^{-1}) may be a more important factor to surpass the CS. Under stable meteorological conditions, a higher formation rate may significantly elevate the possibility that newly formed particles overcome the CS and continuously grow to larger sizes.

3.3   Ion and neutral clusters and further particle growth

During the campaign, we observed and identified different types of ion clusters using the API-ToF, including SA–NH_3, SA–amine, SA–NH_3–amine and SA–NH_3–Org, during NPF events. In Fig. 4a, we presented the mass defect plot of the naturally charged ion clusters on 20 April, when strong NPF events were observed ($J_{1.7}$ of 83 cm^{-3} s^{-1}). The presence of these clusters was usually in conjunction with SA tetramers (SA$_4$), pentamers (SA$_5$) and hexamers (SA$_6$), which potentially contribute to the NPF events. In API-ToF measurement, the absence of alkaline species in the smallest sulfuric acid clusters is likely attributed to the loss of alkaline molecules within the mass spectrometer (Cai et al., 2022; Zha et al., 2023b; Alfaouri et al., 2022).

Among all SA–base (SA–B) clusters, the most abundant SA–NH_3 clusters were from SA$_4$–B to SA$_6$–B (Fig. 4a), even though they are reported to be more easily evaporated than DMA clusters due to collision-induced dissociation (Passananti et al., 2019). Pure SA–amine clusters were only found in the SA$_4$–B clusters with different types of amines, including methylamine (C$_1$–amine), DMA (C$_2$–amine), trimethylamine (C$_3$–amine) and butylamine (C$_4$–amine). The detection of other SA–B besides SA–DMA clusters indicates that other candidate bases could also play a crucial role in the complex atmosphere for nucleation. For example, a recent study conducted in Beijing highlights the importance of TMA, which can increase the nucleation rate from the SA–DMA system by 50 %–100 % (R. Cai et al., 2023). In the Po Valley, the signal intensity of SA$_4$–NH_3 was significantly higher than that of the pure SA$_4$–amine clusters
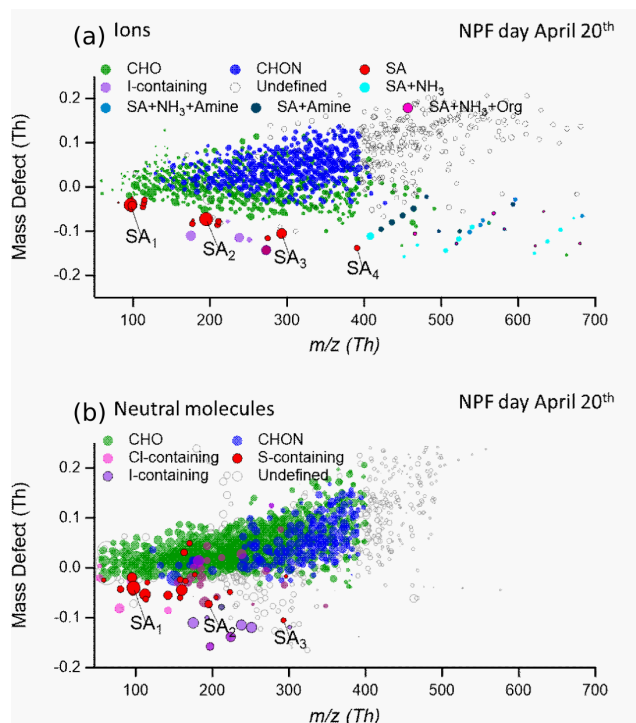
Figure 4. Mass defect plots, which represent the difference between compounds' exact mass and nominal mass, for **(a)** ion clusters and **(b)** neutral clusters during the NPF period (10:00–14:00 LT) on 20 April. The size of the dots is proportional to the logarithm of the signal intensity of each cluster.

(~ 2 times), even though amines (e.g., DMA) were proven to be more efficient (~ 3 orders of magnitude) than NH_3 in clustering (Almeida et al., 2013). $SA–NH_3$–amine clusters could be found along with $SA–NH_3$ clusters in SA_5–B and SA_6–B. Similar patterns of the high fractions of $SA–NH_3$ and $SA–NH_3$–amine clusters were also reported in the CLOUD chamber studies under relatively low-DMA and high-NH_3 conditions (Schobesberger et al., 2013). Therefore, it can be concluded that a large amount of NH_3 also participates in NPF in the Po Valley region. Meanwhile, with a much lower amount, amines also play a crucial role in the formation of small clusters (SA–B) due to their high stabilization efficiencies.

Moreover, some $SA–NH_3$–Org and I-containing ion clusters were also observed on NPF days, although to a much lower extent than clusters involving NH_3 or DMA. It has been shown in previous CLOUD chamber studies that the oxidation products of anthropogenic volatile organic compounds (AVOCs, e.g., naphthalene, trimethylbenzene and toluene) can largely promote the formation rate of particles (Xiao et al., 2021). The I-containing ions (mainly IO_3^-) likely originated from the Adriatic Sea during the daytime. As no large iodine clusters were identified in the APi-ToF (e.g., $(HIO_3)_{0-1}(I_2O_5)_n \cdot IO_3^-$; He et al., 2021), iodine-induced new particle formation in the Po Valley may not be

as important as in the pristine marine environment (Sipila et al., 2016). During NPF without growth days, the formation mechanism was similar to the NPF days with respect to the ion cluster measurement (Fig. S5).

The SA monomer in the Po Valley can be observed during the peak hours (10:00–14:00 LT) on both NPF and non-NPF days, but much lower SA dimer or trimers were found on the non-NPF days (Figs. 4b and S6). At nighttime, the SA concentrations were close to zero due to the scavenging of SO_2 and SA by the high RH (Fig. 1). During our sampling period, large amounts of organics were identified by the CI-APi-ToF. They were typically smaller than 400 Th with carbon numbers < 8 and oxygen numbers < 6 (Fig. S7). Due to the relatively high NO_x levels (13 ppb) that can terminate the dimerization reactions (Yan et al., 2020), no OOM dimers were found, which is different from clean and biogenically dominated environments such as Hyytiälä (Lehtipalo et al., 2018). The compositions of OOMs were similar between NPF and non-NPF days, although with different abundance. Extremely high abundances of nitrophenols and their homologous compounds were found on non-NPF days (~ 8 times higher than on NPF days), likely caused by both the enhanced primary, e.g., biomass burning (Mohr et al., 2013) and pesticide usage (Harrison et al., 2005), and secondary, e.g., photochemical and/or aqueous-phase secondary formation, sources (Zheng et al., 2021; Gilardoni et al., 2016). $C_{2–4}H_{4,5}N_{0,1}O_{3,4}$ compounds were found to be 50 % higher (Fig. S7) on non-NPF days, likely caused by the enhanced heterogeneous reactions that form smaller organics, such as carboxylic acids, under higher-RH conditions. Previous studies have also reported aqueous-phase organic aerosol processing at high RH (Gilardoni et al., 2016) and high concentrations of carboxylic acids, such as formic, oxalic and malonic acids, in the springtime in the Po Valley (Saarikoski et al., 2012). In general, the fraction of the abundance of nitrogen-containing OOMs (CHON) with respect to the total identified OOMs was 60 %–70 %, which is close to the levels reported in polluted cities such as Nanjing (Nie et al., 2022) and Beijing (Guo et al., 2022). A slightly higher fraction of CHON compounds (73 %) was found during non-NPF days than NPF days (67 %), consistent with higher NO_x and fine-particulate-matter levels (Fig. S8). This is likely associated with the stagnant meteorological conditions and the accumulation of pollutants during the non-NPF days. However, the overall high amounts of CHON compounds and the lack of organic dimers make it unlikely that OOMs drive the NPF process (both clustering and initial growth; see, e.g., Simon et al., 2020). Their similar abundance on non-NPF and NPF days was also in line with the similar estimated GR for both types of days.

Throughout the entire sampling period, relatively high concentrations of fine particulate matter (PM$_{2.5}$) were measured, with a daily average of $17 \, \mu g \, m^{-3}$ and a maximum value of $43 \, \mu g \, m^{-3}$. Correspondingly, the hourly CS levels, which quantify the ability of pre-existing particles to

scavenge gaseous precursors, ranged from $< 1 \times 10^{-4}$ to $3 \times 10^{-2} \, \text{s}^{-1}$ with an average value of $5.4 \times 10^{-3} \, \text{s}^{-1}$. Previous studies in polluted areas, such as Chinese megacities, have shown that NPF events are closely linked to CS levels (Cai et al., 2017). The NPF probability was reported to decrease to 50 % when CS was around $1 \times 10^{-2} \, \text{s}^{-1}$ and completely shut off with a CS of $6 \times 10^{-2} \, \text{s}^{-1}$ (Du et al., 2022). However, in the Po Valley, we observed no strong influence of the CS on NPF events, with only a slight difference in the CS during the noontime on non-NPF days (median of $9.4 \times 10^{-3} \, \text{s}^{-1}$) compared with NPF days (median of $8.6 \times 10^{-3} \, \text{s}^{-1}$).

3.4 Comparison between the Po Valley and other environments

Even though the measured $J_{1.7}$ in the Po Valley was at the same level as the values found in polluted Chinese megacities, it was much higher than in clean environments, such as the boreal forest of Hyytiälä in Finland, mountain sites of Jungfraujoch in Switzerland and Chacaltaya in Bolivia ($1.5–2.0 \, \text{cm}^{-3} \, \text{s}^{-1}$; Fig. 5a). The average SA concentrations ($4.6 \times 10^6 \, \text{cm}^{-3}$, 10:00–14:00 LT) were comparable to the levels observed in polluted megacities in China (ranging from 3.9×10^6 to $7.4 \times 10^6 \, \text{cm}^{-3}$; Fig. 5c) but were significantly higher than those in remote areas like Hyytiälä ($9 \times 10^5 \, \text{cm}^{-3}$) and the Jungfraujoch ($5 \times 10^5 \, \text{cm}^{-3}$). SA concentrations during NPF days ($8.6 \times 10^6 \, \text{cm}^{-3}$) in the Po Valley were twice as high as those on non-NPF days ($4 \times 10^6 \, \text{cm}^{-3}$). This difference may be linked to the significant variations (t test, $p < 0.05$) in SO$_2$ concentrations between NPF days (0.38 ppb) and non-NPF days (0.20 ppb). This contrasts with findings in Beijing, where similar or even higher levels of SA and SO$_2$ were observed during non-NPF days compared with NPF event days (Yan et al., 2021). The variations in SO$_2$ and SA concentrations in the Po Valley could possibly be attributed to differences in air masses, as indicated by the higher RH on non-NPF days (53 %) compared with NPF days (38 %) but the similar temperature (NPF days: 288 K; non-NPF days: 287 K). On higher-RH days, photochemistry may be suppressed, potentially reducing the formation of sulfuric acid and low-volatility condensable vapors.

The overall CS in spring (median of $8.9 \times 10^{-3} \, \text{s}^{-1}$) in the Po Valley was lower than that in other polluted cities ($1.5 \times 10^{-1}–2.0 \times 10^{-1} \, \text{s}^{-1}$) but was significantly higher than that in clean environments ($2.0 \times 10^{-4} \, \text{s}^{-1}$ in Hyytiälä and Jungfraujoch to $3.0 \times 10^{-3} \, \text{s}^{-1}$ in Chacaltaya, the latter of which includes the influence of volcanoes) (Fig. 5e). Contrary to Beijing or Shanghai, where CS levels and efficiencies are the dominant factors for the NPF process (Du et al., 2022), NPF events in the Po Valley are not strongly dependent on the CS levels, likely due to generally lower CS levels than the Asian megacities (Fig. S8). The strength of precursor sources and their accumulation in the Po Valley region

might, thus, be more important for NPF to occur than the overall pre-existing sink for those precursors.

The average PM$_1$ concentrations during the sampling period were around $8 \, \mu\text{g} \, \text{m}^{-3}$, significantly lower than Delhi ($269 \, \mu\text{g} \, \text{m}^{-3}$; Mishra et al., 2023) Beijing ($33 \, \mu\text{g} \, \text{m}^{-3}$; Li et al., 2019) and Shanghai ($30 \, \mu\text{g} \, \text{m}^{-3}$; Song et al., 2023) (Fig. S9). The major chemical compositions in PM$_1$ in the Po Valley were similar to those in Beijing and Shanghai, with organics, ammonium nitrate and ammonium sulfate being the most abundant components. However, PM$_1$ compositions in Delhi differed from Po Valley and megacities in China. In Delhi, strong biomass burning emissions with a high abundance of primary organics ($155 \, \mu\text{g} \, \text{m}^{-3}$, 58 %) suppressed NPF events during the daytime from January to February but led to nocturnal particle growth, which is not observed in other polluted areas (Mishra et al., 2023).

Even with the similar CS levels and total PM$_1$ concentrations (NPF: $6.3 \, \mu\text{g} \, \text{m}^{-3}$; non-NPF: $6.5 \, \mu\text{g} \, \text{m}^{-3}$) observed during noontime in the Po Valley, the concentration of NO$_3^-$ increased by 50 % on non-NPF days compared with NPF days, higher than the increase in PM$_1$ (3.1 %) shown in Fig. S9. A lower CS efficiency due to a lower fraction of nitrate was reported to suppress the scavenge of NPF precursors in Beijing (Du et al., 2022), which may also have had a similar influence in the Po Valley. The observed growth rate for 7–15 nm particles in the Po Valley was about $5.1 \, \text{nm} \, \text{h}^{-1}$, comparable to other urban and remote sites ($2.9–9.1 \, \text{nm} \, \text{h}^{-1}$) (Fig. 5f). General similar growth rates among different types of environments have also been reported in previous studies (Deng et al., 2020), requiring further investigation in future research.

For the alkaline gaseous precursors, the average concentration of NH$_3$ was $\sim 10 \, \text{ppb}$, which was in the same range as that found in the Chinese megacities (10–30 ppb) and much higher than those at remote sites ($< 0.1 \, \text{ppb}$) (Table S1 in the Supplement). The high NH$_3$ can be attributed to agricultural treatments, such as fertilization, which were widely applied during springtime in the region. The strong interference of ammonia emitted from fertilization to NPF was also observed in Qvidja, an agricultural site in Southern Finland (Olin et al., 2022). During our sampling period, measured DMA values were too close to the detection limit of the Vocus (Fig. S4), and lower than those observed in the Chinese megacities (10–40 ppt; Fig. 5d). In the spring season, DMA in the Po Valley cannot fully stabilize all atmospheric SA clusters; hence, NPF is very sensitive to variations in the concentrations of the different stabilizers (NH$_3$; DMA; and, as shown by our analysis, likely only to a lower extent, organics). This could explain the scattered correlation between the formation rate and SA concentrations on different days (Fig. 3).

Therefore, in the Po Valley region, the initial nucleation of frequent NPF is primarily attributed to high sulfuric acid concentrations and alkaline molecules, including ammonia and various amines. This mechanism is generally similar to what is observed in Chinese megacities. However, in the Po
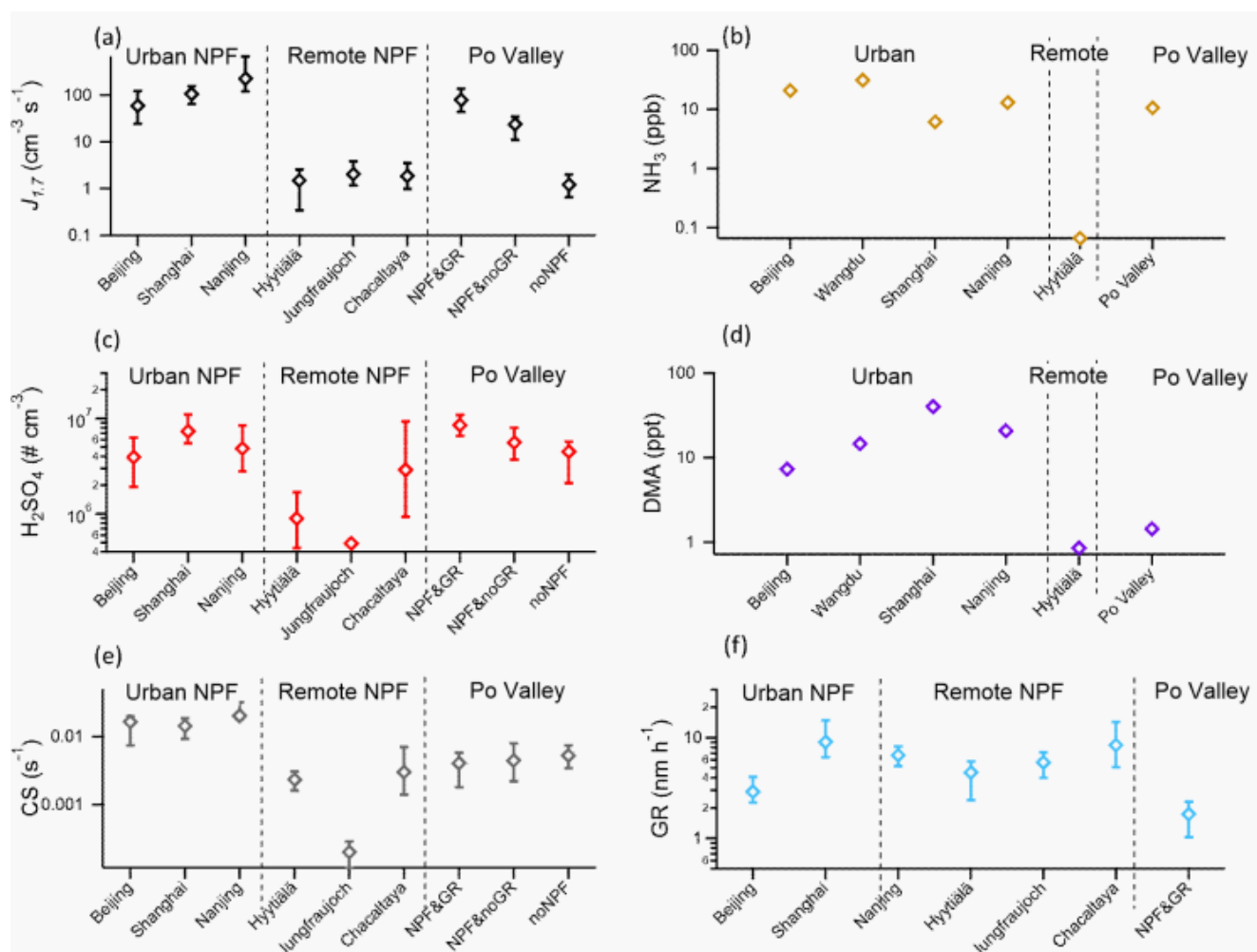
Figure 5. Parameters and gaseous precursors related to NPF in the Po Valley and other environments: **(a)** the formation rate of sub-2 nm particles, **(b)** the atmospheric NH_3 concentrations, **(c)** the SA concentrations, **(d)** the DMA concentrations, **(e)** the CS levels and **(f)** the growth rate in different environments. Diamonds represent the median values; the error bars represent the 25th and 75th percentiles. For the Po Valley data, the formation rates, growth rates, SA concentrations and CS data were selected for 10:00–14:00 LT. The formation rates, growth rates, SA concentrations and CS during NPF in Beijing, Shanghai, Hyytiälä, Jungfraujoch and Chacaltaya are from Deng et al. (2020). The GR calculation range used for comparison varies for different sites: Beijing (GR7–15; Deng et al., 2020), Shanghai (GR7–25; Yao et al., 2018), Nanjing (GR3–20; Yu et al., 2016), Hyytiälä (GR3–20; Vana et al., 2016), Jungfraujoch (GR7–20; Boulon et al., 2010), Chacaltaya (GR7–20; Rose et al., 2015) and Po Valley (GR7–15; this study). The NH_3 and DMA concentrations are from the literature (as listed in the Table S1). Half of the limit of detection (LOD) of DMA concentrations in Hyytiälä was applied in panel **(d)** (Hemmilä et al., 2018). DMA concentrations in the Po Valley were presented as the detection limit reported by Wang et al. (2020) with large uncertainties, as they were not quantified in this study (Fig. S4, Table S1).

Valley region, DMA, a typical base in areas influenced anthropogenic emissions, is insufficient to stabilize the high levels of sulfuric acid, leading to the involvement of other alkaline molecules, such as other type of amines and ammonia, likely originating from fertilization in the area. This involvement of ammonia and other amines differs from Chinese megacities such as Shanghai, where high levels of DMA have been observed (~ 40 ppt; Yao et al., 2016, 2018). As insufficient DMA is available to stabilize all clusters, we speculate that the clustering is therefore sensitive to the abundance of amines. In that sense, during our sampling period, NPF in the Po Valley seems to be more sensitive to the strength of certain emission sources of amines compared with megacity environments, where abundant DMA has been observed. The abundant OOMs dominate the consecutive growth process, leading to a comparable GRs to Chinese megacities such as Beijing and Shanghai. Due to the relatively lower CS than these megacities, however, the newly formed particles may have a higher survival probability and result in more particles

with long-term survival in the Po Valley, indicating a decisive role of NPF in Po Valley aerosol and $PM_{2.5}$ concentrations.

4 Conclusions

In this study, we conducted a continuous 2-month measurement campaign in the Italian Po Valley during springtime, where frequent NPF events were observed on 66 % of all days. Through direct ion cluster measurement, kinetic models and comparison with the CLOUD chamber experiment, we have determined that sulfuric acid–base nucleation is the dominant formation mechanism in the Po Valley region. Abundant sulfuric acid and alkaline molecules, including amines and ammonia derived from agriculture activities, provided ample precursors for NPF events. In contrast to megacity environments, the CS showed no significant difference between NPF event days and non-event days, indicating that it is more the abundance of precursors than the variations in the sink controlling the occurrence of NPF in the Po Valley. Furthermore, we observed that, apart from DMA, a typical basic precursor, NH_3 and other amines were also likely to be involved in NPF in the Po Valley. This was supported by the high abundance of SA–NH_3 and SA–NH_3–amine clusters measured by the APi-ToF during NPF events. DMA, while more efficient than ammonia, was insufficient to stabilize all SA during our sampling period. This resulted in a more scattered correlation between sulfuric acid concentrations and measured formation rates compared with Chinese megacities. In that sense, we could show that the clustering during NPF is clearly distinct between polluted megacity environments and polluted semi-urbanized regions such as the Po Valley. Similar to Beijing, we found that OOMs did not play a decisive role in initial cluster formation, likely due to the absence of ultra-low-volatility organics (typical OOM dimers) in the ion and neutral cluster measurements. However, low-volatility organics were abundant enough to induce fast growth processes above 3 nm. The comparable GRs and formation rates, along with the lower efficient CS compared with megacity environments, indicate a high survival probability for the newly formed particles. Therefore, NPF is likely to play an important role in the fine-particle concentrations and pollution levels in the Po Valley region. Further reductions in key NPF species, including SO_2, amines and NH_3, can contribute to suppressing the NPF event frequency and lowering particle numbers. This, in turn, would improve air quality in the Po Valley region.

Data availability. Data are available from the authors upon request.

Supplement. The supplement related to this article is available online at: https://doi.org/10.5194/acp-24-2423-2024-supplement.

Author contributions. JC, DS, FB and MK designed the research. JC, JS, YFG, SH, MP, AN, FM, SD, MR, NZ and CM collected the data at the SPC site. JC, JS, YG, ST, RY, DA, QZ, DS and FB interpreted the data. MP, WH, YL, GC, LQ, KL, YG, CW, WN, JK, CM, QZ, DS and FB helped to improve the manuscript. JC, JS, DS and FB wrote the manuscript with contributions from all co-authors. All authors have approved the final version of this paper.

Competing interests. At least one of the (co-)authors is a member of the editorial board of *Atmospheric Chemistry and Physics*. The peer-review process was guided by an independent editor, and the authors also have no other competing interests to declare.

Disclaimer. Publisher's note: Copernicus Publications remains neutral with regard to jurisdictional claims made in the text, published maps, institutional affiliations, or any other geographical representation in this paper. While Copernicus Publications makes every effort to include appropriate place names, the final responsibility lies with the authors.

Review statement. This paper was edited by Zhibin Wang and reviewed by Honglei Wang and three anonymous referees.

References

Alfaouri, D., Passananti, M., Zanca, T., Ahonen, L., Kangasluoma, J., Kubečka, J., Myllys, N., and Vehkamäki, H.: A study on the fragmentation of sulfuric acid and dimethylamine clusters inside an atmospheric pressure interface time-of-flight mass spectrometer, Atmos. Meas. Tech., 15, 11–19, https://doi.org/10.5194/amt-15-11-2022, 2022.

Almeida, J., Schobesberger, S., Kurten, A., Ortega, I. K., Kupiainen-Maatta, O., Praplan, A. P., Adamov, A., Amorim, A., Bianchi, F., Breitenlechner, M., David, A., Dommen, J., Donahue, N. M., Downard, A., Dunne, E., Duplissy, J., Ehrhart, S., Flagan, R. C., Franchin, A., Guida, R., Hakala, J., Hansel, A., Heinritzi, M., Henschel, H., Jokinen, T., Junninen, H., Kajos, M., Kangasluoma, J., Keskinen, H., Kupc, A., Kurten, T., Kvashin, A. N., Laaksonen, A., Lehtipalo, K., Leiminger, M., Leppa, J., Loukonen, V., Makhmutov, V., Mathot, S., McGrath, M. J., Nieminen, T., Olenius, T., Onnela, A., Petaja, T., Riccobono, F., Riipinen, I., Rissanen, M., Rondo, L., Ruuskanen, T., Santos, F. D., Sarnela, N., Schallhart, S., Schnitzhofer, R., Seinfeld, J. H., Simon, M., Sipila, M., Stozhkov, Y., Stratmann, F., Tome, A., Trostl, J., Tsagkogeorgas, G., Vaattovaara, P., Viisanen, Y., Virtanen, A., Vrtala, A., Wagner, P. E., Weingartner, E., Wex, H., Williamson, C., Wimmer, D., Ye, P., Yli-Juuti, T., Carslaw, K. S., Kulmala, M., Curtius, J., Baltensperger, U., Worsnop, D. R., Vehkamaki, H., and Kirkby, J.: Molecular understanding of sulphuric acid-amine particle nucleation in the atmosphere, Nature, 502, 359–363, https://doi.org/10.1038/nature12663, 2013.

Brean, J., Beddows, D. C. S., Shi, Z., Temime-Roussel, B., Marchand, N., Querol, X., Alastuey, A., Minguillón, M. C., and Harrison, R. M.: Molecular insights into new particle formation in Barcelona, Spain, Atmos. Chem. Phys., 20, 10029–10045, https://doi.org/10.5194/acp-20-10029-2020, 2020.

Cai, J., Daellenbach, K. R., Wu, C., Zheng, Y., Zheng, F., Du, W., Haslett, S. L., Chen, Q., Kulmala, M., and Mohr, C.: Characterization of offline analysis of particulate matter with FIGAERO-CIMS, Atmos. Meas. Tech., 16, 1147–1165, https://doi.org/10.5194/amt-16-1147-2023, 2023.

Cai, J., Wu, C., Wang, J., Du, W., Zheng, F., Hakala, S., Fan, X., Chu, B., Yao, L., Feng, Z., Liu, Y., Sun, Y., Zheng, J., Yan, C., Bianchi, F., Kulmala, M., Mohr, C., and Daellenbach, K. R.: Influence of organic aerosol molecular composition on particle absorptive properties in autumn Beijing, Atmos. Chem. Phys., 22, 1251–1269, https://doi.org/10.5194/acp-22-1251-2022, 2022.

Cai, R., Yang, D., Fu, Y., Wang, X., Li, X., Ma, Y., Hao, J., Zheng, J., and Jiang, J.: Aerosol surface area concentration: a governing factor in new particle formation in Beijing, Atmos. Chem. Phys., 17, 12327–12340, https://doi.org/10.5194/acp-17-12327-2017, 2017.

Cai, R., Attoui, M., Jiang, J., Korhonen, F., Hao, J., Petäjä, T., and Kangasluoma, J.: Characterization of a high-resolution supercritical differential mobility analyzer at reduced flow rates, Aerosol Sci. Tech., 52, 1332–1343, https://doi.org/10.1080/02786826.2018.1520964, 2018.

Cai, R., Yan, C., Yang, D., Yin, R., Lu, Y., Deng, C., Fu, Y., Ruan, J., Li, X., Kontkanen, J., Zhang, Q., Kangasluoma, J., Ma, Y., Hao, J., Worsnop, D. R., Bianchi, F., Paasonen, P., Kerminen, V. M., Liu, Y., Wang, L., Zheng, J., Kulmala, M., and Jiang, J.: Sulfuric acid–amine nucleation in urban Beijing, Atmos. Chem. Phys., 21, 2457–2468, https://doi.org/10.5194/acp-21-2457-2021, 2021.

Cai, R., Yin, R., Li, X., Xie, H.-B., Yang, D., Kerminen, V.-M., Smith, J. N., Ma, Y., Hao, J., Chen, J., Kulmala, M., Zheng, J., Jiang, J., and Elm, J.: Significant contributions of trimethylamine to sulfuric acid nucleation in polluted environments, npj Clim. Atmos. Sci., 6, 75, https://doi.org/10.1038/s41612-023-00405-3, 2023.

Chu, B., Kerminen, V.-M., Bianchi, F., Yan, C., Petäjä, T., and Kulmala, M.: Atmospheric new particle formation in China, Atmos. Chem. Phys., 19, 115–138, https://doi.org/10.5194/acp-19-115-2019, 2019.

Dada, L., Chellapermal, R., Buenrostro Mazon, S., Paasonen, P., Lampilahti, J., Manninen, H. E., Junninen, H., Petäjä, T., Kerminen, V.-M., and Kulmala, M.: Refined classification and characterization of atmospheric new-particle formation events using air ions, Atmos. Chem. Phys., 18, 17883–17893, https://doi.org/10.5194/acp-18-17883-2018, 2018.

Daellenbach, K. R., Manousakas, M., Jiang, J., Cui, T., Chen, Y., El Haddad, I., Fermo, P., Colombi, C., and Prévôt, A. S. H.: Organic aerosol sources in the Milan metropolitan area – Receptor modelling based on field observations and air quality modelling, Atmos. Environ., 307, 119799, https://doi.org/10.1016/j.atmosenv.2023.119799, 2023.

Dai, L., Wang, H., Zhou, L., An, J., Tang, L., Lu, C., Yan, W., Liu, R., Kong, S., Chen, M., Lee, S., and Yu, H.: Regional and local new particle formation events observed in the Yangtze River Delta region, China, J. Geophys. Res.-Atmos., 122, 2389–2402, https://doi.org/10.1002/2016jd026030, 2017.

Dal Maso, M., Kulmala, M., Riipinen, I., Wagner, R., Hussein, T., Aalto, P. P., and Lehtinen, K. E. J.: Formation and growth of fresh atmospheric aerosols: eight years of aerosol size distribution data from SMEAR II, Hyytiala, Finland, Boreal Environ. Res., 10, 323–336, 2005.

Decesari, S., Allan, J., Plass-Duelmer, C., Williams, B. J., Paglione, M., Facchini, M. C., O'Dowd, C., Harrison, R. M., Gietl, J. K., Coe, H., Giulianelli, L., Gobbi, G. P., Lanconelli, C., Carbone, C., Worsnop, D., Lambe, A. T., Ahern, A. T., Moretti, F., Tagliavini, E., Elste, T., Gilge, S., Zhang, Y., and Dall'Osto, M.: Measurements of the aerosol chemical composition and mixing state in the Po Valley using multiple spectroscopic techniques, Atmos. Chem. Phys., 14, 12109–12132, https://doi.org/10.5194/acp-14-12109-2014, 2014.

de Jesus, A. L., Rahman, M. M., Mazaheri, M., Thompson, H., Knibbs, L. D., Jeong, C., Evans, G., Nei, W., Ding, A., Qiao, L., Li, L., Portin, H., Niemi, J. V., Timonen, H., Luoma, K., Petaja, T., Kulmala, M., Kowalski, M., Peters, A., Cyrys, J., Ferrero, L., Manigrasso, M., Avino, P., Buonano, G., Reche, C., Querol, X., Beddows, D., Harrison, R. M., Sowlat, M. H., Sioutas, C., and Morawska, L.: Ultrafine particles and PM$_{2.5}$ in the air of cities around the world: Are they representative of each other?, Environ. Int., 129, 118–135, https://doi.org/10.1016/j.envint.2019.05.021, 2019.

Deng, C., Fu, Y., Dada, L., Yan, C., Cai, R., Yang, D., Zhou, Y., Yin, R., Lu, Y., Li, X., Qiao, X., Fan, X., Nie, W., Kontkanen, J., Kangasluoma, J., Chu, B., Ding, A., Kerminen, V. M., Paasonen, P., Worsnop, D. R., Bianchi, F., Liu, Y., Zheng, J., Wang, L., Kulmala, M., and Jiang, J.: Seasonal Characteristics of New Particle

Formation and Growth in Urban Beijing, Environ. Sci. Technol., 54, 8547–8557, https://doi.org/10.1021/acs.est.0c00808, 2020.

Du, W., Cai, J., Zheng, F., Yan, C., Zhou, Y., Guo, Y., Chu, B., Yao, L., Heikkinen, L. M., Fan, X., Wang, Y., Cai, R., Hakala, S., Chan, T., Kontkanen, J., Tuovinen, S., Petäjä, T., Kangasluoma, J., Bianchi, F., Paasonen, P., Sun, Y., Kerminen, V.-M., Liu, Y., Daellenbach, K. R., Dada, L., and Kulmala, M.: Influence of Aerosol Chemical Composition on Condensation Sink Efficiency and New Particle Formation in Beijing, Environ. Sci. Technol. Lett., 9, 375–382, https://doi.org/10.1021/acs.estlett.2c00159, 2022.

Fan, X., Cai, J., Yan, C., Zhao, J., Guo, Y., Li, C., Dällenbach, K. R., Zheng, F., Lin, Z., Chu, B., Wang, Y., Dada, L., Zha, Q., Du, W., Kontkanen, J., Kurtén, T., Iyer, S., Kujansuu, J. T., Petäjä, T., Worsnop, D. R., Kerminen, V.-M., Liu, Y., Bianchi, F., Tham, Y. J., Yao, L., and Kulmala, M.: Atmospheric gaseous hydrochloric and hydrobromic acid in urban Beijing, China: detection, source identification and potential atmospheric impacts, Atmos. Chem. Phys., 21, 11437–11452, https://doi.org/10.5194/acp-21-11437-2021, 2021.

Dunne, E. M., Gordon, H., Kürten, A., Almeida, J., Duplissy, J., Williamson, C., Ortega, I. K., Pringle, K. J., Adamov, A., Baltensperger, U., Barme, P., Benduhn, F., Bianchi, F., Breitenlechner, M., Clarke, A., Curtius, J., Dommen, J., Donahue, N. M., Ehrhart, S., Flagan, R. C., Franchin, A., Guida, R., Hakala, J., Hansel, A., Heinritzi, M., Jokinen, T., Kangasluoma, J., Kirkby, J., Kulmala, M., Kupc, A., Lawler, M. J., Lehtipalo, K., Makhmutov, V., Mann, G., Mathot, S., Merikanto, J., Miettinen, P., Nenes, A., Onnela, A., Rap, A., Reddington, C. L. S., Riccobono, F., Richards, N. A. D., Rissanen, M. P., Rondo, L., Sarnela, N., Schobesberger, S., Sengupta, K., Simon, M., Sipilä, M., Smith, J. N., Stozkhov, Y., Tomé, A., Tröstl, J., Wagner, P. E., Wimmer, D., Winkler, P. M., Worsnop, D. R., and Carslaw, K. S.: Global atmospheric particle formation from CERN CLOUD measurements, Science, 354, 1119–1124, https://doi.org/10.1126/science.aaf2649, 2016.

Fernández de la Mora, J. and Kozlowski, J.: Hand-held differential mobility analyzers of high resolution for 1–30 nm particles: Design and fabrication considerations, J. Aerosol Sci., 57, 45-53, https://doi.org/10.1016/j.jaerosci.2012.10.009, 2013.

Finzi, G. and Tebaldi, G.: A mathematical model for air pollution forecast and alarm in an urban area, Atmos. Environ., 16, 2055–2059, https://doi.org/10.1016/0004-6981(82)90276-1, 1982.

Fu, Y., Xue, M., Cai, R., Kangasluoma, J., and Jiang, J.: Theoretical and experimental analysis of the core sampling method: Reducing diffusional losses in aerosol sampling line, Aerosol Sci. Tech., 53, 793–801, https://doi.org/10.1080/02786826.2019.1608354, 2019.

Ge, X., Wexler, A. S., and Clegg, S. L.: Atmospheric amines – Part I. A review, Atmos. Environ., 45, 524–546, https://doi.org/10.1016/j.atmosenv.2010.10.012, 2011.

Gilardoni, S., Massoli, P., Paglione, M., Giulianelli, L., Carbone, C., Rinaldi, M., Decesari, S., Sandrini, S., Costabile, F., Gobbi, G. P., Pietrogrande, M. C., Visentin, M., Scotto, F., Fuzzi, S., and Facchini, M. C.: Direct observation of aqueous secondary organic aerosol from biomass-burning emissions, P. Natl. Acad. Sci. USA, 113, 10013–10018, https://doi.org/10.1073/pnas.1602212113, 2016.

Guo, S., Hu, M., Zamora, M. L., Peng, J., Shang, D., Zheng, J., Du, Z., Wu, Z., Shao, M., Zeng, L., Molina, M. J., and Zhang, R.: Elucidating severe urban haze formation in China, P. Natl. Acad. Sci. USA, 111, 17373–17378, https://doi.org/10.1073/pnas.1419604111, 2014.

Guo, S., Hu, M., Peng, J., Wu, Z., Zamora, M. L., Shang, D., Du, Z., Zheng, J., Fang, X., Tang, R., Wu, Y., Zeng, L., Shuai, S., Zhang, W., Wang, Y., Ji, Y., Li, Y., Zhang, A. L., Wang, W., Zhang, F., Zhao, J., Gong, X., Wang, C., Molina, M. J., and Zhang, R.: Remarkable nucleation and growth of ultrafine particles from vehicular exhaust, P. Natl. Acad. Sci. USA, 117, 3427–3432, https://doi.org/10.1073/pnas.1916366117, 2020.

Guo, Y., Yan, C., Liu, Y., Qiao, X., Zheng, F., Zhang, Y., Zhou, Y., Li, C., Fan, X., Lin, Z., Feng, Z., Zhang, Y., Zheng, P., Tian, L., Nie, W., Wang, Z., Huang, D., Daellenbach, K. R., Yao, L., Dada, L., Bianchi, F., Jiang, J., Liu, Y., Kerminen, V.-M., and Kulmala, M.: Seasonal variation in oxygenated organic molecules in urban Beijing and their contribution to secondary organic aerosol, Atmos. Chem. Phys., 22, 10077–10097, https://doi.org/10.5194/acp-22-10077-2022, 2022.

Hamed, A., Joutsensaari, J., Mikkonen, S., Sogacheva, L., Dal Maso, M., Kulmala, M., Cavalli, F., Fuzzi, S., Facchini, M. C., Decesari, S., Mircea, M., Lehtinen, K. E. J., and Laaksonen, A.: Nucleation and growth of new particles in Po Valley, Italy, Atmos. Chem. Phys., 7, 355–376, https://doi.org/10.5194/acp-7-355-2007, 2007.

Harrison, M. A. J., Barra, S., Borghesi, D., Vione, D., Arsene, C., and Iulian Olariu, R.: Nitrated phenols in the atmosphere: a review, Atmospheric Environment, 39, 231-248, 10.1016/j.atmosenv.2004.09.044, 2005.

He, X. C., Tham, Y. J., Dada, L., Wang, M., Finkenzeller, H., Stolzenburg, D., Iyer, S., Simon, M., Kurten, A., Shen, J., Rorup, B., Rissanen, M., Schobesberger, S., Baalbaki, R., Wang, D. S., Koenig, T. K., Jokinen, T., Sarnela, N., Beck, L. J., Almeida, J., Amanatidis, S., Amorim, A., Ataei, F., Baccarini, A., Bertozzi, B., Bianchi, F., Brilke, S., Caudillo, L., Chen, D., Chiu, R., Chu, B., Dias, A., Ding, A., Dommen, J., Duplissy, J., El Haddad, I., Gonzalez Carracedo, L., Granzin, M., Hansel, A., Heinritzi, M., Hofbauer, V., Junninen, H., Kangasluoma, J., Kemppainen, D., Kim, C., Kong, W., Krechmer, J. E., Kvashin, A., Laitinen, T., Lamkaddam, H., Lee, C. P., Lehtipalo, K., Leiminger, M., Li, Z., Makhmutov, V., Manninen, H. E., Marie, G., Marten, R., Mathot, S., Mauldin, R. L., Mentler, B., Mohler, O., Muller, T., Nie, W., Onnela, A., Petaja, T., Pfeifer, J., Philippov, M., Ranjithkumar, A., Saiz-Lopez, A., Salma, I., Scholz, W., Schuchmann, S., Schulze, B., Steiner, G., Stozhkov, Y., Tauber, C., Tome, A., Thakur, R. C., Vaisanen, O., Vazquez-Pufleau, M., Wagner, A. C., Wang, Y., Weber, S. K., Winkler, P. M., Wu, Y., Xiao, M., Yan, C., Ye, Q., Ylisirnio, A., Zauner-Wieczorek, M., Zha, Q., Zhou, P., Flagan, R. C., Curtius, J., Baltensperger, U., Kulmala, M., Kerminen, V. M., Kurten, T., Donahue, N. M., Volkamer, R., Kirkby, J., Worsnop, D. R., and Sipila, M.: Role of iodine oxoacids in atmospheric aerosol nucleation, Science, 371, 589–595, https://doi.org/10.1126/science.abe0298, 2021.

Hemmilä, M., Hellén, H., Virkkula, A., Makkonen, U., Praplan, A. P., Kontkanen, J., Ahonen, L., Kulmala, M., and Hakola, H.: Amines in boreal forest air at SMEAR II station in Finland, Atmos. Chem. Phys., 18, 6367–6380, https://doi.org/10.5194/acp-18-6367-2018, 2018.

Jokinen, T., Sipilä, M., Junninen, H., Ehn, M., Lönn, G., Hakala, J., Petäjä, T., Mauldin, R. L., Kulmala, M., and Worsnop, D. R.: Atmospheric sulphuric acid and neutral cluster measurements using CI-APi-TOF, Atmos. Chem. Phys., 12, 4117–4125, https://doi.org/10.5194/acp-12-4117-2012, 2012.

Junninen, H., Ehn, M., Petäjä, T., Luosujärvi, L., Kotiaho, T., Kostiainen, R., Rohner, U., Gonin, M., Fuhrer, K., Kulmala, M., and Worsnop, D. R.: A high-resolution mass spectrometer to measure atmospheric ion composition, Atmos. Meas. Tech., 3, 1039–1053, https://doi.org/10.5194/amt-3-1039-2010, 2010.

Kangasluoma, J., Attoui, M., Junninen, H., Lehtipalo, K., Samodurov, A., Korhonen, F., Sarnela, N., Schmidt-Ott, A., Worsnop, D., Kulmala, M., and Petäjä, T.: Sizing of neutral sub 3nm tungsten oxide clusters using Airmodus Particle Size Magnifier, J. Aerosol Sci., 87, 53–62, https://doi.org/10.1016/j.jaerosci.2015.05.007, 2015.

Kangasluoma, J., Franchin, A., Duplissy, J., Ahonen, L., Korhonen, F., Attoui, M., Mikkilä, J., Lehtipalo, K., Vanhanen, J., Kulmala, M., and Petäjä, T.: Operation of the Airmodus A11 nano Condensation Nucleus Counter at various inlet pressures and various operation temperatures, and design of a new inlet system, Atmos. Meas. Tech., 9, 2977–2988, https://doi.org/10.5194/amt-9-2977-2016, 2016.

Kangasluoma, J., Ahonen, L. R., Laurila, T. M., Cai, R., Enroth, J., Mazon, S. B., Korhonen, F., Aalto, P. P., Kulmala, M., Attoui, M., and Petäjä, T.: Laboratory verification of a new high flow differential mobility particle sizer, and field measurements in Hyytiälä, J. Aerosol Sci., 124, 1–9, https://doi.org/10.1016/j.jaerosci.2018.06.009, 2018.

Kirkby, J., Curtius, J., Almeida, J., Dunne, E., Duplissy, J., Ehrhart, S., Franchin, A., Gagne, S., Ickes, L., Kurten, A., Kupc, A., Metzger, A., Riccobono, F., Rondo, L., Schobesberger, S., Tsagkogeorgas, G., Wimmer, D., Amorim, A., Bianchi, F., Breitenlechner, M., David, A., Dommen, J., Downard, A., Ehn, M., Flagan, R. C., Haider, S., Hansel, A., Hauser, D., Jud, W., Junninen, H., Kreissl, F., Kvashin, A., Laaksonen, A., Lehtipalo, K., Lima, J., Lovejoy, E. R., Makhmutov, V., Mathot, S., Mikkila, J., Minginette, P., Mogo, S., Nieminen, T., Onnela, A., Pereira, P., Petaja, T., Schnitzhofer, R., Seinfeld, J. H., Sipila, M., Stozhkov, Y., Stratmann, F., Tome, A., Vanhanen, J., Viisanen, Y., Vrtala, A., Wagner, P. E., Walther, H., Weingartner, E., Wex, H., Winkler, P. M., Carslaw, K. S., Worsnop, D. R., Baltensperger, U., and Kulmala, M.: Role of sulphuric acid, ammonia and galactic cosmic rays in atmospheric aerosol nucleation, Nature, 476, 429–433, https://doi.org/10.1038/nature10343, 2011.

Kirkby, J., Duplissy, J., Sengupta, K., Frege, C., Gordon, H., Williamson, C., Heinritzi, M., Simon, M., Yan, C., Almeida, J., Trostl, J., Nieminen, T., Ortega, I. K., Wagner, R., Adamov, A., Amorim, A., Bernhammer, A. K., Bianchi, F., Breitenlechner, M., Brilke, S., Chen, X., Craven, J., Dias, A., Ehrhart, S., Flagan, R. C., Franchin, A., Fuchs, C., Guida, R., Hakala, J., Hoyle, C. R., Jokinen, T., Junninen, H., Kangasluoma, J., Kim, J., Krapf, M., Kurten, A., Laaksonen, A., Lehtipalo, K., Makhmutov, V., Mathot, S., Molteni, U., Onnela, A., Perakyla, O., Piel, F., Petaja, T., Praplan, A. P., Pringle, K., Rap, A., Richards, N. A., Riipinen, I., Rissanen, M. P., Rondo, L., Sarnela, N., Schobesberger, S., Scott, C. E., Seinfeld, J. H., Sipila, M., Steiner, G., Stozhkov, Y., Stratmann, F., Tome, A., Virtanen, A., Vogel, A. L., Wagner, A. C., Wagner, P. E., Weingartner, E., Wimmer, D., Winkler,

P. M., Ye, P., Zhang, X., Hansel, A., Dommen, J., Donahue, N. M., Worsnop, D. R., Baltensperger, U., Kulmala, M., Carslaw, K. S., and Curtius, J.: Ion-induced nucleation of pure biogenic particles, Nature, 533, 521–526, https://doi.org/10.1038/nature17953, 2016.

Kontkanen, J., Järvinen, E., Manninen, H. E., Lehtipalo, K., Kangasluoma, J., Decesari, S., Gobbi, G. P., Laaksonen, A., Petäjä, T., and Kulmala, M.: High concentrations of sub-3nm clusters and frequent new particle formation observed in the Po Valley, Italy, during the PEGASOS 2012 campaign, Atmos. Chem. Phys., 16, 1919–1935, https://doi.org/10.5194/acp-16-1919-2016, 2016.

Kontkanen, J., Lehtipalo, K., Ahonen, L., Kangasluoma, J., Manninen, H. E., Hakala, J., Rose, C., Sellegri, K., Xiao, S., Wang, L., Qi, X., Nie, W., Ding, A., Yu, H., Lee, S., Kerminen, V.-M., Petäjä, T., and Kulmala, M.: Measurements of sub-3 nm particles using a particle size magnifier in different environments: from clean mountain top to polluted megacities, Atmos. Chem. Phys., 17, 2163–2187, https://doi.org/10.5194/acp-17-2163-2017, 2017.

Krechmer, J., Lopez-Hilfiker, F., Koss, A., Hutterli, M., Stoermer, C., Deming, B., Kimmel, J., Warneke, C., Holzinger, R., Jayne, J., Worsnop, D., Fuhrer, K., Gonin, K., and de Gouw, J.: Evaluation of a New Reagent-Ion Source and Focusing Ion–Molecule Reactor for Use in Proton-Transfer-Reaction Mass Spectrometry, Anal. Chem., 90, 12011–12018, https://doi.org/10.1021/acs.analchem.8b02641, 2018.

Kulmala, M., Petäjä, T., Nieminen, T., Sipilä, M., Manninen, H. E., Lehtipalo, K., Dal Maso, M., Aalto, P. P., Junninen, H., Paasonen, P., Riipinen, I., Lehtinen, K. E. J., Laaksonen, A., and Kerminen, V.-M.: Measurement of the nucleation of atmospheric aerosol particles, Nat. Protoc., 7, 1651–1667, https://doi.org/10.1038/nprot.2012.091, 2012.

Kulmala, M., Kontkanen, J., Junninen, H., Lehtipalo, K., Manninen, H. E., Nieminen, T., Petäjä, T., Sipilä, M., Schobesberger, S., Rantala, P., Franchin, A., Jokinen, T., Järvinen, E., Äijälä, M., Kangasluoma, J., Hakala, J., Aalto, P. P., Paasonen, P., Mikkilä, J., Vanhanen, J., Aalto, J., Hakola, H., Makkonen, U., Ruuskanen, T., Mauldin, R. L., Duplissy, J., Vehkamäki, H., Bäck, J., Kortelainen, A., Riipinen, I., Kurtén, T., Johnston, M. V., Smith, J. N., Ehn, M., Mentel, T. F., Lehtinen, K. E. J., Laaksonen, A., Kerminen, V.-M., and Worsnop, D. R.: Direct Observations of Atmospheric Aerosol Nucleation, Science, 339, 943–946, https://doi.org/10.1126/science.1227385, 2013.

Kulmala, M., Kerminen, V. M., Petäjä, T., Ding, A. J., and Wang, L.: Atmospheric gas-to-particle conversion: why NPF events are observed in megacities?, Faraday Discuss., 200, 271–288, https://doi.org/10.1039/C6FD00257A, 2017.

Kulmala, M., Dada, L., Daellenbach, K. R., Yan, C., Stolzenburg, D., Kontkanen, J., Ezhova, E., Hakala, S., Tuovinen, S., Kokkonen, T. V., Kurppa, M., Cai, R., Zhou, Y., Yin, R., Baalbaki, R., Chan, T., Chu, B., Deng, C., Fu, Y., Ge, M., He, H., Heikkinen, L., Junninen, H., Liu, Y., Lu, Y., Nie, W., Rusanen, A., Vakkari, V., Wang, Y., Yang, G., Yao, L., Zheng, J., Kujansuu, J., Kangasluoma, J., Petaja, T., Paasonen, P., Jarvi, L., Worsnop, D., Ding, A., Liu, Y., Wang, L., Jiang, J., Bianchi, F., and Kerminen, V. M.: Is reducing new particle formation a plausible solution to mitigate particulate air pollution in Beijing

and other Chinese megacities?, Faraday Discuss., 226, 334–347, https://doi.org/10.1039/d0fd00078g, 2021.

Kulmala, M., Junninen, H., Dada, L., Salma, I., Weidinger, T., Thén, W., Vörösmarty, M., Komsaare, K., Stolzenburg, D., Cai, R., Yan, C., Li, X., Deng, C., Jiang, J., Petäjä, T., Nieminen, T., and Kerminen, V.-M.: Quiet New Particle Formation in the Atmosphere, Front. Environ. Sci., 10, 912385, https://doi.org/10.3389/fenvs.2022.912385, 2022.

Kurten, A., Rondo, L., Ehrhart, S., and Curtius, J.: Calibration of a chemical ionization mass spectrometer for the measurement of gaseous sulfuric acid, J. Phys. Chem. A, 116, 6375–6386, https://doi.org/10.1021/jp212123n, 2012.

Lampimäki, M., Baalbaki, R., Ahonen, L., Korhonen, F., Cai, R., Chan, T., Stolzenburg, D., Petäjä, T., Kangasluoma, J., Vanhanen, J., and Lehtipalo, K.: Novel aerosol diluter – Size dependent characterization down to 1 nm particle size, J. Aerosol Sci., 172, 106180, https://doi.org/10.1016/j.jaerosci.2023.106180, 2023.

Lehtipalo, K., Yan, C., Dada, L., Bianchi, F., Xiao, M., Wagner, R., Stolzenburg, D., Ahonen, L. R., Amorim, A., Baccarini, A., Bauer, P. S., Baumgartner, B., Bergen, A., Bernhammer, A.-K., Breitenlechner, M., Brilke, S., Buchholz, A., Mazon, S. B., Chen, D., Chen, X., Dias, A., Dommen, J., Draper, D. C., Duplissy, J., Ehn, M., Finkenzeller, H., Fischer, L., Frege, C., Fuchs, C., Garmash, O., Gordon, H., Hakala, J., He, X., Heikkinen, L., Heinritzi, M., Helm, J. C., Hofbauer, V., Hoyle, C. R., Jokinen, T., Kangasluoma, J., Kerminen, V.-M., Kim, C., Kirkby, J., Kontkanen, J., Kürten, A., Lawler, M. J., Mai, H., Mathot, S., Mauldin, R. L., Molteni, U., Nichman, L., Nie, W., Nieminen, T., Ojdanic, A., Onnela, A., Passananti, M., Petäjä, T., Piel, F., Pospisilova, V., Quéléver, L. L. J., Rissanen, M. P., Rose, C., Sarnela, N., Schallhart, S., Schuchmann, S., Sengupta, K., Simon, M., Sipilä, M., Tauber, C., Tomé, A., Tröstl, J., Väisänen, O., Vogel, A. L., Volkamer, R., Wagner, A. C., Wang, M., Weitz, L., Wimmer, D., Ye, P., Ylisirniö, A., Zha, Q., Carslaw, K. S., Curtius, J., Donahue, N. M., Flagan, R. C., Hansel, A., Riipinen, I., Virtanen, A., Winkler, P. M., Baltensperger, U., Kulmala, M., and Worsnop, D. R.: Multicomponent new particle formation from sulfuric acid, ammonia, and biogenic vapors, Sci. Adv., 4, eaau5363, https://doi.org/10.1126/sciadv.aau5363, 2018.

Lehtipalo, K., Ahonen, L. R., Baalbaki, R., Sulo, J., Chan, T., Laurila, T., Dada, L., Duplissy, J., Miettinen, E., Vanhanen, J., Kangasluoma, J., Kulmala, M., Petäjä, T., and Jokinen, T.: The standard operating procedure for Airmodus Particle Size Magnifier and nano-Condensation Nucleus Counter, J. Aerosol Sci., 159, 105896, https://doi.org/10.1016/j.jaerosci.2021.105896, 2022.

Leng, C., Kish, J. D., Roberts, J. E., Dwebi, I., Chon, N., and Liu, Y.: Temperature-Dependent Henry's Law Constants of Atmospheric Amines, J. Phys. Chem. A, 119, 8884–8891, https://doi.org/10.1021/acs.jpca.5b05174, 2015.

Li, H., Cheng, J., Zhang, Q., Zheng, B., Zhang, Y., Zheng, G., and He, K.: Rapid transition in winter aerosol composition in Beijing from 2014 to 2017: response to clean air actions, Atmos. Chem. Phys., 19, 11485–11499, https://doi.org/10.5194/acp-19-11485-2019, 2019.

Li, X., Rohrer, F., Hofzumahaus, A., Brauers, T., Häseler, R., Bohn, B., Broch, S., Fuchs, H., Gomm, S., Holland, F., Jäger, J., Kaiser, J., Keutsch, F. N., Lohse, I., Lu, K., Tillmann, R., Wegener, R., Wolfe, G. M., Mentel, T. F., Kiendler-Scharr, A., and Wahner, A.: Missing Gas-Phase Source of HONO Inferred from Zep-

pelin Measurements in the Troposphere, Sciencs, 1344, 292–296, https://doi.org/0.1126/science.1248999, 2014.

Liu, S., Hu, M., Wu, Z., Wehner, B., Wiedensohler, A., and Cheng, Y.: Aerosol number size distribution and new particle formation at a rural/coastal site in Pearl River Delta (PRD) of China, Atmos. Environ., 42, 6275–6283, https://doi.org/10.1016/j.atmosenv.2008.01.063, 2008.

Manninen, H. E., Nieminen, T., Asmi, E., Gagné, S., Häkkinen, S., Lehtipalo, K., Aalto, P., Vana, M., Mirme, A., Mirme, S., Hõrrak, U., Plass-Dülmer, C., Stange, G., Kiss, G., Hoffer, A., Törő, N., Moerman, M., Henzing, B., de Leeuw, G., Brinkenberg, M., Kouvarakis, G. N., Bougiatioti, A., Mihalopoulos, N., O'Dowd, C., Ceburnis, D., Arneth, A., Svenningsson, B., Swietlicki, E., Tarozzi, L., Decesari, S., Facchini, M. C., Birmili, W., Sonntag, A., Wiedensohler, A., Boulon, J., Sellegri, K., Laj, P., Gysel, M., Bukowiecki, N., Weingartner, E., Wehrle, G., Laaksonen, A., Hamed, A., Joutsensaari, J., Petäjä, T., Kerminen, V. M., and Kulmala, M.: EUCAARI ion spectrometer measurements at 12 European sites – analysis of new particle formation events, Atmos. Chem. Phys., 10, 7907–7927, https://doi.org/10.5194/acp-10-7907-2010, 2010.

Mishra, S., Tripathi, S. N., Kanawade, V. P., Haslett, S. L., Dada, L., Ciarelli, G., Kumar, V., Singh, A., Bhattu, D., Rastogi, N., Daellenbach, K. R., Ganguly, D., Gargava, P., Slowik, J. G., Kulmala, M., Mohr, C., El-Haddad, I., and Prevot, A. S. H.: Rapid night-time nanoparticle growth in Delhi driven by biomass-burning emissions, Nat. Geosci., 16, 224–230, https://doi.org/10.1038/s41561-023-01138-x, 2023.

Mohr, C., Lopez-Hilfiker, F. D., Zotter, P., Prevot, A. S., Xu, L., Ng, N. L., Herndon, S. C., Williams, L. R., Franklin, J. P., Zahniser, M. S., Worsnop, D. R., Knighton, W. B., Aiken, A. C., Gorkowski, K. J., Dubey, M. K., Allan, J. D., and Thornton, J. A.: Contribution of nitrated phenols to wood burning brown carbon light absorption in Detling, United Kingdom during winter time, Environ. Sci. Technol., 47, 6316–6324, https://doi.org/10.1021/es400683v, 2013.

Nie, W., Yan, C., Huang, D. D., Wang, Z., Liu, Y., Qiao, X., Guo, Y., Tian, L., Zheng, P., Xu, Z., Li, Y., Xu, Z., Qi, X., Sun, P., Wang, J., Zheng, F., Li, X., Yin, R., Dallenbach, K. R., Bianchi, F., Petäjä, T., Zhang, Y., Wang, M., Schervish, M., Wang, S., Qiao, L., Wang, Q., Zhou, M., Wang, H., Yu, C., Yao, D., Guo, H., Ye, P., Lee, S., Li, Y. J., Liu, Y., Chi, X., Kerminen, V.-M., Ehn, M., Donahue, N. M., Wang, T., Huang, C., Kulmala, M., Worsnop, D., Jiang, J., and Ding, A.: Secondary organic aerosol formed by condensing anthropogenic vapours over China's megacities, Nat. Geosci., 15, 255–261, https://doi.org/10.1038/s41561-022-00922-5, 2022.

Olin, M., Okuljar, M., Rissanen, M. P., Kalliokoski, J., Shen, J., Dada, L., Lampimäki, M., Wu, Y., Lohila, A., Duplissy, J., Sipilä, M., Petäjä, T., Kulmala, M., and Dal Maso, M.: Measurement report: Atmospheric new particle formation in a coastal agricultural site explained with binPMF analysis of nitrate CI-APi-TOF spectra, Atmos. Chem. Phys., 22, 8097–8115, https://doi.org/10.5194/acp-22-8097-2022, 2022.

Paasonen, P., Nieminen, T., Asmi, E., Manninen, H. E., Petäjä, T., Plass-Dülmer, C., Flentje, H., Birmili, W., Wiedensohler, A., Hõrrak, U., Metzger, A., Hamed, A., Laaksonen, A., Facchini, M. C., Kerminen, V. M., and Kulmala, M.: On the roles of sulphuric acid and low-volatility organic vapours in the ini-

tial steps of atmospheric new particle formation, Atmos. Chem. Phys., 10, 11223–11242, https://doi.org/10.5194/acp-10-11223-2010, 2010.

Paglione, M., Saarikoski, S., Carbone, S., Hillamo, R., Facchini, M. C., Finessi, E., Giulianelli, L., Carbone, C., Fuzzi, S., Moretti, F., Tagliavini, E., Swietlicki, E., Eriksson Stenström, K., Prévôt, A. S. H., Massoli, P., Canaragatna, M., Worsnop, D., and Decesari, S.: Primary and secondary biomass burning aerosols determined by proton nuclear magnetic resonance (<sup>1</sup>H-NMR) spectroscopy during the 2008 EUCAARI campaign in the Po Valley (Italy), Atmos. Chem. Phys., 14, 5089–5110, https://doi.org/10.5194/acp-14-5089-2014, 2014.

Paglione, M., Gilardoni, S., Rinaldi, M., Decesari, S., Zanca, N., Sandrini, S., Giulianelli, L., Bacco, D., Ferrari, S., Poluzzi, V., Scotto, F., Trentini, A., Poulain, L., Herrmann, H., Wiedensohler, A., Canonaco, F., Prévôt, A. S. H., Massoli, P., Carbone, C., Facchini, M. C., and Fuzzi, S.: The impact of biomass burning and aqueous-phase processing on air quality: a multi-year source apportionment study in the Po Valley, Italy, Atmos. Chem. Phys., 20, 1233–1254, https://doi.org/10.5194/acp-20-1233-2020, 2020.

Paglione, M., Decesari, S., Rinaldi, M., Tarozzi, L., Manarini, F., Gilardoni, S., Facchini, M. C., Fuzzi, S., Bacco, D., Trentini, A., Pandis, S. N., and Nenes, A.: Historical Changes in Seasonal Aerosol Acidity in the Po Valley (Italy) as Inferred from Fog Water and Aerosol Measurements, Environ. Sci. Technol., 55, 7307–7315, https://doi.org/10.1021/acs.est.1c00651, 2021.

Passananti, M., Zapadinsky, E., Zanca, T., Kangasluoma, J., Myllys, N., Rissanen, M. P., Kurten, T., Ehn, M., Attoui, M., and Vehkamaki, H.: How well can we predict cluster fragmentation inside a mass spectrometer?, Chem. Commun., 55, 5946–5949, https://doi.org/10.1039/c9cc02896j, 2019.

Peineke, C., Attoui, M. B., and Schmidt-Ott, A.: Using a glowing wire generator for production of charged, uniformly sized nanoparticles at high concentrations, J. Aerosol Sci., 37, 1651–1661, https://doi.org/10.1016/j.jaerosci.2006.06.006, 2006.

Peng, J. F., Hu, M., Wang, Z. B., Huang, X. F., Kumar, P., Wu, Z. J., Guo, S., Yue, D. L., Shang, D. J., Zheng, Z., and He, L. Y.: Submicron aerosols at thirteen diversified sites in China: size distribution, new particle formation and corresponding contribution to cloud condensation nuclei production, Atmos. Chem. Phys., 14, 10249–10265, https://doi.org/10.5194/acp-14-10249-2014, 2014.

Saarikoski, S., Carbone, S., Decesari, S., Giulianelli, L., Angelini, F., Canagaratna, M., Ng, N. L., Trimborn, A., Facchini, M. C., Fuzzi, S., Hillamo, R., and Worsnop, D.: Chemical characterization of springtime submicrometer aerosol in Po Valley, Italy, Atmos. Chem. Phys., 12, 8401–8421, https://doi.org/10.5194/acp-12-8401-2012, 2012.

Schobesberger, S., Junninen, H., Bianchi, F., Lonn, G., Ehn, M., Lehtipalo, K., Dommen, J., Ehrhart, S., Ortega, I. K., Franchin, A., Nieminen, T., Riccobono, F., Hutterli, M., Duplissy, J., Almeida, J., Amorim, A., Breitenlechner, M., Downard, A. J., Dunne, E. M., Flagan, R. C., Kajos, M., Keskinen, H., Kirkby, J., Kupc, A., Kurten, A., Kurten, T., Laaksonen, A., Mathot, S., Onnela, A., Praplan, A. P., Rondo, L., Santos, F. D., Schallhart, S., Schnitzhofer, R., Sipila, M., Tome, A., Tsagkogeorgas, G., Vehkamaki, H., Wimmer, D., Baltensperger, U., Carslaw, K.

S., Curtius, J., Hansel, A., Petaja, T., Kulmala, M., Donahue, N. M., and Worsnop, D. R.: Molecular understanding of atmospheric particle formation from sulfuric acid and large oxidized organic molecules, P. Natl. Acad. Sci. USA, 110, 17223–17228, https://doi.org/10.1073/pnas.1306973110, 2013.

Schraufnagel, D. E.: The health effects of ultrafine particles, Exp. Mol. Med., 52, 311–317, https://doi.org/10.1038/s12276-020-0403-3, 2020.

Sebastian, M., Kompalli, S. K., Kumar, V. A., Jose, S., Babu, S. S., Pandithurai, G., Singh, S., Hooda, R. K., Soni, V. K., Pierce, J. R., Vakkari, V., Asmi, E., Westervelt, D. M., Hyvärinen, A.-P., and Kanawade, V. P.: Observations of particle number size distributions and new particle formation in six Indian locations, Atmos. Chem. Phys., 22, 4491–4508, https://doi.org/10.5194/acp-22-4491-2022, 2022.

Shen, J., Bigi, A., Marinoni, A., Lampilahti, J., Kontkanen, J., Ciarelli, G., Putaud, J. P., Nieminen, T., Kulmala, M., Lehtipalo, K., and Bianchi, F.: Emerging Investigator Series: COVID-19 lockdown effects on aerosol particle size distributions in northern Italy, Environ. Sci. Atmos., 1, 214–227, https://doi.org/10.1039/d1ea00016k, 2021.

Shen, X. J., Sun, J. Y., Zhang, Y. M., Wehner, B., Nowak, A., Tuch, T., Zhang, X. C., Wang, T. T., Zhou, H. G., Zhang, X. L., Dong, F., Birmili, W., and Wiedensohler, A.: First long-term study of particle number size distributions and new particle formation events of regional aerosol in the North China Plain, Atmos. Chem. Phys., 11, 1565–1580, https://doi.org/10.5194/acp-11-1565-2011, 2011.

Simon, M., Dada, L., Heinritzi, M., Scholz, W., Stolzenburg, D., Fischer, L., Wagner, A. C., Kürten, A., Rörup, B., He, X.-C., Almeida, J., Baalbaki, R., Baccarini, A., Bauer, P. S., Beck, L., Bergen, A., Bianchi, F., Bräkling, S., Brilke, S., Caudillo, L., Chen, D., Chu, B., Dias, A., Draper, D. C., Duplissy, J., El-Haddad, I., Finkenzeller, H., Frege, C., Gonzalez-Carracedo, L., Gordon, H., Granzin, M., Hakala, J., Hofbauer, V., Hoyle, C. R., Kim, C., Kong, W., Lamkaddam, H., Lee, C. P., Lehtipalo, K., Leiminger, M., Mai, H., Manninen, H. E., Marie, G., Marten, R., Mentler, B., Molteni, U., Nichman, L., Nie, W., Ojdanic, A., Onnela, A., Partoll, E., Petäjä, T., Pfeifer, J., Philippov, M., Quéléver, L. L. J., Ranjithkumar, A., Rissanen, M. P., Schallhart, S., Schobesberger, S., Schuchmann, S., Shen, J., Sipilä, M., Steiner, G., Stozhkov, Y., Tauber, C., Tham, Y. J., Tomé, A. R., Vazquez-Pufleau, M., Vogel, A. L., Wagner, R., Wang, M., Wang, D. S., Wang, Y., Weber, S. K., Wu, Y., Xiao, M., Yan, C., Ye, P., Ye, Q., Zauner-Wieczorek, M., Zhou, X., Baltensperger, U., Dommen, J., Flagan, R. C., Hansel, A., Kulmala, M., Volkamer, R., Winkler, P. M., Worsnop, D. R., Donahue, N. M., Kirkby, J., and Curtius, J.: Molecular understanding of new-particle formation from α-pinene between -50 and $+25$ °C, Atmos. Chem. Phys., 20, 9183–9207, https://doi.org/10.5194/acp-20-9183-2020, 2020.

Sipila, M., Sarnela, N., Jokinen, T., Henschel, H., Junninen, H., Kontkanen, J., Richters, S., Kangasluoma, J., Franchin, A., Perakyla, O., Rissanen, M. P., Ehn, M., Vehkamaki, H., Kurten, T., Berndt, T., Petaja, T., Worsnop, D., Ceburnis, D., Kerminen, V. M., Kulmala, M., and O'Dowd, C.: Molecular-scale evidence of aerosol particle formation via sequential addition of HIO_3, Nature, 537, 532–534, https://doi.org/10.1038/nature19314, 2016.

Song, Z., Gao, W., Shen, H., Jin, Y., Zhang, C., Luo, H., Pan, L., Yao, B., Zhang, Y., Huo, J., Sun, Y., Yu, D., Chen, H., Chen, J., Duan, Y., Zhao, D., and Xu, J.: Roles of Regional Transport and Vertical Mixing in Aerosol Pollution in Shanghai Over the COVID-19 Lockdown Period Observed Above Urban Canopy, J. Geophys. Res.-Atmos., 128, e2023JD038540, https://doi.org/10.1029/2023JD038540, 2023.

Stolzenburg, D., Fischer, L., Vogel, A. L., Heinritzi, M., Schervish, M., Simon, M., Wagner, A. C., Dada, L., Ahonen, L. R., Amorim, A., Baccarini, A., Bauer, P. S., Baumgartner, B., Bergen, A., Bianchi, F., Breitenlechner, M., Brilke, S., Buenrostro Mazon, S., Chen, D., Dias, A., Draper, D. C., Duplissy, J., El Haddad, I., Finkenzeller, H., Frege, C., Fuchs, C., Garmash, O., Gordon, H., He, X., Helm, J., Hofbauer, V., Hoyle, C. R., Kim, C., Kirkby, J., Kontkanen, J., Kurten, A., Lampilahti, J., Lawler, M., Lehtipalo, K., Leiminger, M., Mai, H., Mathot, S., Mentler, B., Molteni, U., Nie, W., Nieminen, T., Nowak, J. B., Ojdanic, A., Onnela, A., Passananti, M., Petaja, T., Quelever, L. L. J., Rissanen, M. P., Sarnela, N., Schallhart, S., Tauber, C., Tome, A., Wagner, R., Wang, M., Weitz, L., Wimmer, D., Xiao, M., Yan, C., Ye, P., Zha, Q., Baltensperger, U., Curtius, J., Dommen, J., Flagan, R. C., Kulmala, M., Smith, J. N., Worsnop, D. R., Hansel, A., Donahue, N. M., and Winkler, P. M.: Rapid growth of organic aerosol nanoparticles over a wide tropospheric temperature range, P. Natl. Acad. Sci. USA, 115, 9122–9127, https://doi.org/10.1073/pnas.1807604115, 2018.

Stolzenburg, D., Simon, M., Ranjithkumar, A., Kürten, A., Lehtipalo, K., Gordon, H., Ehrhart, S., Finkenzeller, H., Pichelstorfer, L., Nieminen, T., He, X.-C., Brilke, S., Xiao, M., Amorim, A., Baalbaki, R., Baccarini, A., Beck, L., Bräkling, S., Caudillo Murillo, L., Chen, D., Chu, B., Dada, L., Dias, A., Dommen, J., Duplissy, J., El Haddad, I., Fischer, L., Gonzalez Carracedo, L., Heinritzi, M., Kim, C., Koenig, T. K., Kong, W., Lamkaddam, H., Lee, C. P., Leiminger, M., Li, Z., Makhmutov, V., Manninen, H. E., Marie, G., Marten, R., Müller, T., Nie, W., Partoll, E., Petäjä, T., Pfeifer, J., Philippov, M., Rissanen, M. P., Rörup, B., Schobesberger, S., Schuchmann, S., Shen, J., Sipilä, M., Steiner, G., Stozhkov, Y., Tauber, C., Tham, Y. J., Tomé, A., Vazquez-Pufleau, M., Wagner, A. C., Wang, M., Wang, Y., Weber, S. K., Wimmer, D., Wlasits, P. J., Wu, Y., Ye, Q., Zauner-Wieczorek, M., Baltensperger, U., Carslaw, K. S., Curtius, J., Donahue, N. M., Flagan, R. C., Hansel, A., Kulmala, M., Lelieveld, J., Volkamer, R., Kirkby, J., and Winkler, P. M.: Enhanced growth rate of atmospheric particles from sulfuric acid, Atmos. Chem. Phys., 20, 7359–7372, https://doi.org/10.5194/acp-20-7359-2020, 2020.

Ude, S. and de la Mora, J. F.: Molecular monodisperse mobility and mass standards from electrosprays of tetraalkyl ammonium halides, J. Aerosol Sci., 36, 1224–1237, https://doi.org/10.1016/j.jaerosci.2005.02.009, 2005.

Vanhanen, J., Mikkilä, J., Lehtipalo, K., Sipilä, M., Manninen, H. E., Siivola, E., Petäjä, T., and Kulmala, M.: Particle Size Magnifier for Nano-CN Detection, Aerosol Sci. Tech., 45, 533–542, https://doi.org/10.1080/02786826.2010.547889, 2011.

Wang, Y., Yang, G., Lu, Y., Liu, Y., Chen, J., and Wang, L.: Detection of gaseous dimethylamine using vocus proton-transfer-reaction time-of-flight mass spectrometry, Atmos. Environ., 243, 117875, https://doi.org/10.1016/j.atmosenv.2020.117875, 2020.

Wang, Z., Wu, Z., Yue, D., Shang, D., Guo, S., Sun, J., Ding, A., Wang, L., Jiang, J., Guo, H., Gao, J., Cheung, H. C., Morawska, L., Keywood, M., and Hu, M.: New particle formation in China: Current knowledge and further directions, Sci. Total Environ., 577, 258–266, https://doi.org/10.1016/j.scitotenv.2016.10.177, 2017.

Wang, Z. B., Hu, M., Sun, J. Y., Wu, Z. J., Yue, D. L., Shen, X. J., Zhang, Y. M., Pei, X. Y., Cheng, Y. F., and Wiedensohler, A.: Characteristics of regional new particle formation in urban and regional background environments in the North China Plain, Atmos. Chem. Phys., 13, 12495–12506, https://doi.org/10.5194/acp-13-12495-2013, 2013.

Wang, Z. B., Hu, M., Pei, X. Y., Zhang, R. Y., Paasonen, P., Zheng, J., Yue, D. L., Wu, Z. J., Boy, M., and Wiedensohler, A.: Connection of organics to atmospheric new particle formation and growth at an urban site of Beijing, Atmos. Environ., 103, 7–17, https://doi.org/10.1016/j.atmosenv.2014.11.069, 2015.

Wu, Z., Hu, M., Liu, S., Wehner, B., Bauer, S., Ma ßling, A., Wiedensohler, A., Petäjä, T., Dal Maso, M., and Kulmala, M.: New particle formation in Beijing, China: Statistical analysis of a 1-year data set, J. Geophys. Res., 112, D09209, https://doi.org/10.1029/2006jd007406, 2007.

Wu, Z., Hu, M., Yue, D., Wehner, B., and Wiedensohler, A.: Evolution of particle number size distribution in an urban atmosphere during episodes of heavy pollution and new particle formation, Sci. China Earth Sci., 54, 1772–1778, https://doi.org/10.1007/s11430-011-4227-9, 2011.

Xiao, M., Hoyle, C. R., Dada, L., Stolzenburg, D., Kürten, A., Wang, M., Lamkaddam, H., Garmash, O., Mentler, B., Molteni, U., Baccarini, A., Simon, M., He, X.-C., Lehtipalo, K., Ahonen, L. R., Baalbaki, R., Bauer, P. S., Beck, L., Bell, D., Bianchi, F., Brilke, S., Chen, D., Chiu, R., Dias, A., Duplissy, J., Finkenzeller, H., Gordon, H., Hofbauer, V., Kim, C., Koenig, T. K., Lampilahti, J., Lee, C. P., Li, Z., Mai, H., Makhmutov, V., Manninen, H. E., Marten, R., Mathot, S., Mauldin, R. L., Nie, W., Onnela, A., Partoll, E., Petäjä, T., Pfeifer, J., Pospisilova, V., Quéléver, L. L. J., Rissanen, M., Schobesberger, S., Schuchmann, S., Stozhkov, Y., Tauber, C., Tham, Y. J., Tomé, A., Vazquez-Pufleau, M., Wagner, A. C., Wagner, R., Wang, Y., Weitz, L., Wimmer, D., Wu, Y., Yan, C., Ye, P., Ye, Q., Zha, Q., Zhou, X., Amorim, A., Carslaw, K., Curtius, J., Hansel, A., Volkamer, R., Winkler, P. M., Flagan, R. C., Kulmala, M., Worsnop, D. R., Kirkby, J., Donahue, N. M., Baltensperger, U., El Haddad, I., and Dommen, J.: The driving factors of new particle formation and growth in the polluted boundary layer, Atmos. Chem. Phys., 21, 14275–14291, https://doi.org/10.5194/acp-21-14275-2021, 2021.

Xiao, S., Wang, M. Y., Yao, L., Kulmala, M., Zhou, B., Yang, X., Chen, J. M., Wang, D. F., Fu, Q. Y., Worsnop, D. R., and Wang, L.: Strong atmospheric new particle formation in winter in urban Shanghai, China, Atmos. Chem. Phys., 15, 1769–1781, https://doi.org/10.5194/acp-15-1769-2015, 2015.

Yan, C., Nie, W., Vogel, A. L., Dada, L., Lehtipalo, K., Stolzenburg, D., Wagner, R., Rissanen, M. P., Xiao, M., Ahonen, L., Fischer, L., Rose, C., Bianchi, F., Gordon, H., Simon, M., Heinritzi, M., Garmash, O., Roldin, P., Dias, A., Ye, P., Hofbauer, V., Amorim, A., Bauer, P. S., Bergen, A., Bernhammer, A.-K., Breitenlechner, M., Brilke, S., Buchholz, A., Mazon, S. B., Canagaratna, M. R., Chen, X., Ding, A., Dommen, J., Draper, D. C., Duplissy, J.,

Frege, C., Heyn, C., Guida, R., Hakala, J., Heikkinen, L., Hoyle, C. R., Jokinen, T., Kangasluoma, J., Kirkby, J., Kontkanen, J., Kürten, A., Lawler, M. J., Mai, H., Mathot, S., Mauldin, R. L., Molteni, U., Nichman, L., Nieminen, T., Nowak, J., Ojdanic, A., Onnela, A., Pajunoja, A., Petäjä, T., Piel, F., Quéléver, L. L. J., Sarnela, N., Schallhart, S., Sengupta, K., Sipilä, M., Tomé, A., Tröstl, J., Väisänen, O., Wagner, A. C., Ylisirniö, A., Zha, Q., Baltensperger, U., Carslaw, K. S., Curtius, J., Flagan, R. C., Hansel, A., Riipinen, I., Smith, J. N., Virtanen, A., Winkler, P. M., Donahue, N. M., Kerminen, V.-M., Kulmala, M., Ehn, M., and Worsnop, D. R.: Size-dependent influence of $NO_x r$ on the growth rates of organic aerosol particles, Sci. Adv., 6, eaay4945, https://doi.org/10.1126/sciadv.aay4945, 2020.

Yan, C., Yin, R., Lu, Y., Dada, L., Yang, D., Fu, Y., Kontkanen, J., Deng, C., Garmash, O., Ruan, J., Baalbaki, R., Schervish, M., Cai, R., Bloss, M., Chan, T., Chen, T., Chen, Q., Chen, X., Chen, Y., Chu, B., Dällenbach, K., Foreback, B., He, X., Heikkinen, L., Jokinen, T., Junninen, H., Kangasluoma, J., Kokkonen, T., Kurppa, M., Lehtipalo, K., Li, H., Li, H., Li, X., Liu, Y., Ma, Q., Paasonen, P., Rantala, P., Pileci, R. E., Rusanen, A., Sarnela, N., Simonen, P., Wang, S., Wang, W., Wang, Y., Xue, M., Yang, G., Yao, L., Zhou, Y., Kujansuu, J., Petäjä, T., Nie, W., Ma, Y., Ge, M., He, H., Donahue, N. M., Worsnop, D. R., Veli-Matti, K., Wang, L., Liu, Y., Zheng, J., Kulmala, M., Jiang, J., and Bianchi, F.: The Synergistic Role of Sulfuric Acid, Bases, and Oxidized Organics Governing New-Particle Formation in Beijing, Geophys. Res. Lett., 48, e2020GL091944, https://doi.org/10.1029/2020gl091944, 2021.

Yao, L., Wang, M.-Y., Wang, X.-K., Liu, Y.-J., Chen, H.-F., Zheng, J., Nie, W., Ding, A.-J., Geng, F.-H., Wang, D.-F., Chen, J.-M., Worsnop, D. R., and Wang, L.: Detection of atmospheric gaseous amines and amides by a high-resolution time-of-flight chemical ionization mass spectrometer with protonated ethanol reagent ions, Atmos. Chem. Phys., 16, 14527–14543, https://doi.org/10.5194/acp-16-14527-2016, 2016.

Yao, L., Garmash, O., Bianchi, F., Zheng, J., Yan, C., Kontkanen, J., Junninen, H., Mazon, S. B., Ehn, M., Paasonen, P., Sipila, M., Wang, M. Y., Wang, X. K., Xiao, S., Chen, H. F., Lu, Y. Q., Zhang, B. W., Wang, D. F., Fu, Q. Y., Geng, F. H., Li, L., Wang, H. L., Qiao, L. P., Yang, X., Chen, J. M., Kerminen, V. M., Petaja, T., Worsnop, D. R., Kulmala, M., and Wang, L.: Atmospheric new particle formation from sulfuric acid and amines in a Chinese megacity, Science, 361, 278–281, https://doi.org/10.1126/science.aao4839, 2018.

Yu, H., Zhou, L., Dai, L., Shen, W., Dai, W., Zheng, J., Ma, Y., and Chen, M.: Nucleation and growth of sub-3 nm particles in the polluted urban atmosphere of a megacity in China, Atmos. Chem. Phys., 16, 2641–2657, https://doi.org/10.5194/acp-16-2641-2016, 2016.

Yue, D. L., Hu, M., Wang, Z. B., Wen, M. T., Guo, S., Zhong, L. J., Wiedensohler, A., and Zhang, Y. H.: Comparison of particle number size distributions and new particle formation between the urban and rural sites in the PRD region, China, Atmos. Environ., 76, 181-188, https://doi.org/10.1016/j.atmosenv.2012.11.018, 2013.

Zha, Q., Yan, C., Junninen, H., Riva, M., Sarnela, N., Aalto, J., Quéléver, L., Schallhart, S., Dada, L., Heikkinen, L., Peräkylä, O., Zou, J., Rose, C., Wang, Y., Mammarella, I., Katul, G., Vesala, T., Worsnop, D. R., Kulmala, M., Petäjä, T., Bianchi, F., and Ehn, M.: Vertical characterization of highly oxygenated molecules (HOMs) below and above a boreal forest canopy, Atmos. Chem. Phys., 18, 17437–17450, https://doi.org/10.5194/acp-18-17437-2018, 2018.

Zha, Q., Huang, W., Aliaga, D., Peräkylä, O., Heikkinen, L., Koenig, A. M., Wu, C., Enroth, J., Gramlich, Y., Cai, J., Carbone, S., Hansel, A., Petäjä, T., Kulmala, M., Worsnop, D., Sinclair, V., Krejci, R., Andrade, M., Mohr, C., and Bianchi, F.: Measurement report: Molecular-level investigation of atmospheric cluster ions at the tropical high-altitude research station Chacaltaya (524 m a.s.l.) in the Bolivian Andes, Atmos. Chem. Phys., 23, 4559–4576, https://doi.org/10.5194/acp-23-4559-2023, 2023a.

Zha, Q., Aliaga, D., Krejci, R., Sinclair, V., Wu, C., Ciarelli, G., Scholz, W., Heikkinen, L., Partoll, E., Gramlich, Y., Huang, W., Leiminger, M., Enroth, J., Peräkylä, O., Cai, R., Chen, X., Koenig, A. M., Velarde, F., Moreno, I., Petäjä, T., Artaxo, P., Laj, P., Hansel, A., Carbone, S., Kulmala, M., Andrade, M., Worsnop, D., Mohr, C., and Bianchi, F.: Oxidized organic molecules in the tropical free troposphere over Amazonia, Natl. Sci. Rev., 11, nwad138, https://doi.org/10.1093/nsr/nwad138, 2023b.

Zheng, Y., Chen, Q., Cheng, X., Mohr, C., Cai, J., Huang, W., Shrivastava, M., Ye, P., Fu, P., Shi, X., Ge, Y., Liao, K., Miao, R., Qiu, X., Koenig, T. K., and Chen, S.: Precursors and Pathways Leading to Enhanced Secondary Organic Aerosol Formation during Severe Haze Episodes, Environ. Sci. Technol., 55, 15680–15693, https://doi.org/10.1021/acs.est.1c04255, 2021.

Zhu, S., Yan, C., Zheng, J., Chen, C., Ning, H., Yang, D., Wang, M., Ma, Y., Zhan, J., Hua, C., Yin, R., Li, Y., Liu, Y., Jiang, J., Yao, L., Wang, L., Kulmala, M., and Worsnop, D. R.: Observation and Source Apportionment of Atmospheric Alkaline Gases in Urban Beijing, Environ. Sci. Technol., 56, 17545–17555, https://doi.org/10.1021/acs.est.2c03584, 2022.